

# Systemic Risk in a Unifying Framework for Cascading Processes on Networks

Jan Lorenz, Stefano Battiston, Frank Schweitzer

Chair of Systems Design, ETH Zurich, Kreuzplatz 5, 8032 Zurich, Switzerland

## Abstract

We introduce a general framework for models of cascade and contagion processes on networks, to identify their commonalities and differences. In particular, models of social and financial cascades, as well as the fiber bundle model, the voter model, and models of epidemic spreading are recovered as special cases. To unify their description, we define the net fragility of a node, which is the difference between its fragility and the threshold that determines its failure. Nodes fail if their net fragility grows above zero and their failure increases the fragility of neighbouring nodes, thus possibly triggering a cascade. In this framework, we identify three classes depending on the way the fragility of a node is increased by the failure of a neighbour. At the microscopic level, we illustrate with specific examples how the failure spreading pattern varies with the node triggering the cascade, depending on its position in the network and its degree. At the macroscopic level, systemic risk is measured as the final fraction of failed nodes,  $X^*$ , and for each of the three classes we derive a recursive equation to compute its value. The phase diagram of  $X^*$  as a function of the initial conditions, thus allows for a prediction of the systemic risk as well as a comparison of the three different model classes. We could identify which model class lead to a first-order phase transition in systemic risk, i.e. situations where small changes in the initial conditions may lead to a global failure. Eventually, we generalize our framework to encompass stochastic contagion models. This indicates the potential for further generalizations.

**PACS:** 64.60.aq Networks, 89.65.Gh Economics; econophysics, financial markets, business and management, 87.23.Ge Dynamics of social systems, 62.20.M- Structural failure of materials

## 1 Introduction

After the spread of the financial crisis in 2008, the term 'systemic risk' could be well regarded as the buzzword of these years. Although there is no consensus on a formal definition of systemic risk, it usually denotes the risk that a whole system, consisting of many interacting agents, fails. These agents, in an economic context, could be firms, banks, funds, or other institutions. Only very recently, financial economics is accepting the idea that the relation between robustness of individual institutions and systemic risk is not necessarily straightforward [24]. The debate on systemic risk, how it originates and how it is affected by the structure of the networks of financial contracts among institutions worldwide, is only at the beginning [6, 22]. From the point of view

of economic networks, systemic risk can even be conceived as an undesired externality arising from the strategic interaction of the agents [28]. However, systemic risk is not only a financial or economic issue, it also appears in other social and technical systems. The spread of infectious diseases, the blackout of a power network, or the rupture of a fiber bundle are just some examples. Systemic risk – in our perspective – is a macroscopic property of a system which emerges due to the nonlinear interactions of agents on a microscopic level. As in many other problems in statistical physics, the question is how such a macroscopic property may emerge from local interactions, given some specific boundary conditions of the system. The main research question is then to predict the fraction of failed nodes  $X$  in a system, either as a time dependent quantity or in equilibrium. Here, we regard  $X$  as a measure of systemic risk.

In this paper we investigate systemic risk from a complex network perspective. Thus, agents are represented by nodes and interactions by directed and weighted links of a network. Each of the nodes is characterized by two discrete states  $\{0, 1\}$ , which can be interpreted as a susceptible and an infected state or, equivalently, as a healthy and a failed state. In most situations considered here, the failure (infection) of a node exerts some form of stress on the neighbouring nodes which can possibly cause the failure (infection) of the neighbours, this way triggering a cascade, which means that node after node fails. This may happen via a redistribution mechanism, in which part of the stress acting on a node is transferred to neighboring nodes, which assumes that the total stress is conserved. There is another mechanism, however, where no such conserved quantity exist, for example in infection processes where the disease can be transferred to an unlimited number of nodes. In both mechanisms, the likelihood that a node fails increases with the number of failures in the proximity of the node. This is the essence of a contagion process. The specific dynamics may vary across applications, nevertheless there are common features which should be pointed out and systematically investigated. Our paper contributes to this task by developing a general framework which encompass most of the existing models and allows to classify cascade models in three different categories.

A number of works have investigated processes of this type, sometimes referred to as 'cascades' or 'contagion'. These were mostly dealing with interacting units with random mixing or, more recently, with fixed interaction structures corresponding to complex networks. On the one hand, there are models in which the failure dynamics is deterministic but the threshold, at which such a failure happens, is heterogeneous across nodes. For simplicity, we refer to these as *cascade models* – even though, according to the discussion above, they also involve contagion. To this class belong some early works on electrical breakdown in random networks [17] and more recent ones on the fiber bundle model (FBM) [31, 23, 18], on fractures [9], cascades in power grids [7], or cascades in sand piles – the Bak-Tang-Wiesenfeld model (BTW) [13]. Further work refers to congestion dynamics in networks, [4], cascades in financial systems [2] and in social interactions [35], and overload distribution (in abstract terms) [25]. The properties of self-organized criticality

of some of these models are well understood [34, 8]. The presence of rare but large avalanches is of course relevant to systemic risk [30].

On the other hand, there are models in which the failure of a given node is stochastic but the threshold at which contagion takes place is homogeneous across nodes. For simplicity, we refer to this class as *contagion models*, even though they can lead to cascades as well. The best known example is epidemic spreading (SIS) [26] [33]. The properties of these model have been investigated in great detail on various network topologies, e.g. in the presence of correlations [5] or bipartite structure [14]. However, as we will see later, we can also include the voter model (VM) and its variants [32, 27] into this class. It is interesting to note that, while the macroscopic behaviour of FBM and BTW in a scale free topology is qualitatively similar to the one on regular and random graphs, the properties of SIS are severely affected by the topology. The relation between cascading models and contagion models has not been investigated in depth, although some models interpolating between the two classes have been proposed [10, 11]

To relate these two model classes of cascades and contagion, in the following we develop a general model of cascades on networks where nodes are characterized by a two continuous variables, *fragility* and *threshold*. Nodes fail if their fragility exceed their individual heterogeneous threshold. The key variable is the net fragility  $z$ , i.e. the difference between fragility and threshold. This variable is related to the notion of 'distance to default' used in financial economics [1]. By specifying the the fragility of a node in terms of other nodes fragility and/or other nodes failure state, we are able to recover various existing cascade models. In particular, we identify three classes of cascade models, referred to as 'constant load', 'load redistribution', 'overload redistribution'. The three classes differ, given that a node fails, in how the increase in fragility (called here the 'load') of connected nodes is specified. We discuss the differences and similarities among these classes also with respect to models from financial economics and sociology. For all of the three classes we derive mean-field recursive equation for the asymptotic fraction of failed nodes,  $X^*$ . Clearly, this variable depends on the initial distributions of both fragility and threshold across nodes. For instance, if no node is fragile enough to fail in the beginning, then no cascade is triggered. We thus compare how different models behave depending on the mean and variance of the initial distribution of  $z$  across nodes.

As a further contribution, we extend the general framework to encompass models of stochastic contagion. In such a framework, the failure of a given node is a stochastic event depending both on the state of neighbourhood and on the individual threshold. We derive a general equation for the expected change of the fraction of failed nodes, from which one can recover the usual mean-field equations of the SIS model, but interestingly also of the VM, as special cases.

Our work wishes to contribute to a better understanding of the relations between cascading models, contagion models and herding models on networks, from the point of view of systemic risk.

## 2 A Framework for Deterministic Models of Cascades

In this section we develop a general framework to describe cascading processes on a network. This framework will be extended in Sec. 5 to encompass also stochastic contagion models. On the microscopic side, we characterize each node  $i$  of the network at time  $t$  by a dynamic variable  $s_i(t) \in \{0, 1\}$  characterizing the failure state. The state is  $s_i(t) = 1$  if the node has failed and  $s_i(t) = 0$  otherwise. Other metaphors apply equally well to our model, e.g. ‘infected/healthy’, ‘immune/susceptible’, or ‘broken/in function’. On the macroscopic side, the system state at time  $t$  is encoded in the  $n$ -dimensional state vector  $s(t)$ , with  $n$  being the number of nodes. The macrodynamic variable of interest for systemic risk is the total *fraction of failed nodes* in the system

$$X(t) = \frac{1}{n} \sum_{i=1}^n s_i(t). \quad (1)$$

If values of  $X(t)$  close to one are reached the system is prone to systemic risk. When trajectories always stay close to zero the system is free of systemic risk. For simplicity, in the following, we will consider models which converge in  $X(t)$  to stationary states  $X^*$ . So, the *final fraction of failed nodes*  $X^*$  is our proxy for the systemic risk of the system.

In order to describe various existing models in a single framework, we assume that the failure state  $s_i(t)$  of each node is, in turn, determined by a continuous variable  $\phi_i(t)$ , representing the *fragility* of the node. A node remains healthy as long as  $\phi_i(t) < \theta_i$ , where the constant parameter  $\theta_i$  represents the *threshold* above which the fragility determines the failure. Conversely, the node fails if  $\phi_i(t) \geq \theta$ . In other words,

$$s_i(t+1) = \Theta(z_i(t)) , \text{ with } z_i(t) = \phi_i(t) - \theta_i \quad (2)$$

where  $\Theta$  is the Heaviside function (here meant to be  $\Theta(z) = 0$  if  $z < 0$  and  $\Theta(z) = 1$  if  $z \geq 0$ ). The variable  $z_i(t)$  is called *net fragility*. As it is defined as the difference between fragility and failing threshold its absolute value has the same meaning of *distance to default* in finance, for  $z \leq 0$  [1]. Notice that in the equation above time runs in discrete steps, consistently with failure being a discrete event.

This general framework can be applied to different models by specifying the functional form of fragility. As we will see, depending on the case under consideration,  $\phi_i(t)$  can be a function of the failure state vector  $s(t)$  and some static parameters, such as the network structure and the initial distribution of stress on the nodes. It can also be a function of the vector of fragility  $\phi(t-1)$  at previous times. The latter constitutes a coupled system with the vectors  $s(t)$  and  $\phi(t)$  as state variables. In any case, fragility depends on the current failure state and determines the new failures at the next time step. Thus, cascades are triggered by the fact that failures induce other failures. Specific models will be described in Sec. 3

The interaction among nodes is specified by the (possibly weighted) adjacency matrix of the network  $A \in \mathbb{R}^{n \times n}$ , with  $a_{ij} \geq 0$ . For specific models some restrictions to the adjacency matrix may apply, e.g. one may consider undirected links, no self-links or some condition on the weights. In this framework the adjacency matrix of the network influences the dynamics only as a static parameter, i.e., we do not consider feedbacks from the state of a node on the link structure as in [20].

If we assume a large number of nodes, it makes sense to look at the distribution of the net fragility  $z(t)$ , in terms of its density function  $p_{z(t)}$ . Then from Eqn. 1 and 2 it follows that the fraction of failed nodes at the next time step is given by

$$X(t+1) = \int_0^\infty p_{z(t)}(z) dz = 1 - \int_{-\infty}^0 p_{z(t)}(z) dz. \quad (3)$$

In the cascading process new failures modify over time the values of fragility of other nodes. We can also formulate the dynamics in the space of density functions:

$$p_{z(t+1)} = \mathcal{F}(p_{z(t)}). \quad (4)$$

If we know both the density function  $p_{\phi(t)}$  of the fragility at time  $t$  and the density function  $p_\theta$  of the failing threshold, we can write

$$\begin{aligned} p_{z(t)}(z) &= p_{\phi(t)-\theta}(z) = (p_{\phi(t)} * p_{-\theta})(z) \\ &= \int p_{\phi(t)}(y) * p_\theta(y-z) dy \end{aligned} \quad (5)$$

with ‘\*’ denoting the convolution. The expression above assumes that fragility and threshold are stochastically independent across nodes. Depending on the specific model, the functional operator  $\mathcal{F}$ , in Eqn. (4), may also include dependencies on other static parameters. The general idea is to find a density  $p_{z^*}$  that is an attractive fix point of  $\mathcal{F}$ , so that the asymptotic fraction of failed nodes  $X^*$  is obtained via Eqn. (3).

### 3 Specific Cascading Models

In many cascading processes on networks, the failure of a node causes a redistribution of load, stress or damage to the neighbouring nodes. In our framework, such redistribution of load can be seen as if a failure causes an increase of fragility in the neighbours. In the following, we distinguish three different classes of models, denoted as (i) ‘constant load’, (ii) ‘load redistribution’, and (iii) ‘overload redistribution’. We keep the term ‘load’ because it is more intuitive. We will show how these model classes are described in our unifying framework in terms of fragility and

threshold, and how some models known in the literature fit into these classes. The differences in the cascading process across the models will be illustrated by taking the small undirected network of Figure 1 as an example. For each model, we consider the same initial configuration

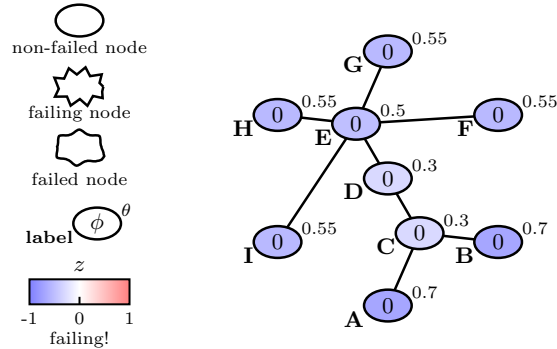


Figure 1: Initial configuration of the generic example used to illustrate all models. The legend is valid for all further graphs of this type. The discrete state  $s_i$  is represented by the shape of the node. A healthy node has  $s_i = 0$ , a failed one  $s_i = 1$ . A failing node is a node with  $s_i = 0$  but  $z_i > 0$ , so it will switch to the failed state in the next time step. Nodes are labeled with capital letters. The level of fragility  $\phi_i$  (which changes over time) is indicated inside each node. The failing threshold  $\theta_i$  (constant over time) is indicated as superscript to the node. The color code specified in the colorbar refers to the value of net fragility  $z_i = \phi_i - \theta_i$ .

with respect to the net fragility  $z_i(0)$  in which all nodes are healthy (i.e. with  $z_i(0)$  negative). During the first time step, the value  $z_C$  of node C is perturbed so that it fails. The subsequent time steps reveal how the propagation of failure occurs in the different models.

### 3.1 Models with Constant Load

Model class (i) (‘constant load’) assumes that the failure of a node  $i$  causes a predetermined increase of fragility to its neighbours. The term ‘constant’ does not imply that the increase is uniform for all nodes (on the contrary, some nodes may receive more load than others). It means that the increase in the fragility of node  $i$ , when its neighbor  $j$  fails, is the same regardless of the fragility of  $j$  and of the situation in the rest of the system.

We can now distinguish two cases. In the first case, the increase in fragility of a node  $i$  is proportional to the fraction of neighbors that fail. This is a reasonable assumption if the ties in the network represent for instance financial dependencies or social influence. In the second case, the increase in fragility of a node  $i$ , when neighbor  $j$  fails, is inversely proportional to the number of neighbors of node  $j$ . In other words, the load of  $j$  is shared equally among the neighbours and thus the more are its neighbours, the smaller is the additional load that each one, including  $i$ , has

to carry. We will refer to the first case as the *inward variant* of the model because the increase in fragility caused by the failure of one neighbour depends only on the in-degree of the node receiving the load. In contrast, we will refer to the second case as the *outward variant*, because the increase in fragility depends only on the out-degree of the failing node.

We now start by casting in our framework the well known threshold model of collective behavior by Granovetter [15]. The model was developed in the context of social unrest, with people going on riot when the fraction of the population which is already on riot exceeds a given individual activation threshold. This model has been more recently repropsoed as generic model of cascades on networks [35].

We assume an initial vector of failing thresholds  $\theta$ , and initial failing states  $s_i(0) = 0$  for all  $i$ . We define fragility as simply the fraction of failed neighbors,

$$\phi_i(t) = \frac{1}{k_i^{\text{in}}} \sum_{j \in \text{nb}_{\text{in}}(i,A)} s_j(t), \quad (6)$$

with  $\text{nb}_{\text{in}}(i, A)$  being the set of all in-neighbors of  $i$  in the network  $A$  and  $k_i^{\text{in}}$  being the cardinality of the set (i.e. the in-degree of  $i$ ). This means that a node fails when the fraction of its failed neighbors exceeds its failing threshold. Consequently, the initial fragility across nodes is zero  $\phi_i(0) = 0$  for all  $i$  and the dynamical equation (2) implies  $s(1) = \Theta(-\theta)$ . Thus, nodes with negative threshold correspond to initial failures at time step  $t = 1$ .

Interestingly, we can map our inward cascading model with constant load also to an economic model of bankruptcy cascades introduced in [3]. In that model firms are connected in a network of credit and supply relations. Each firm  $i$  is characterised by a financial robustness  $\rho_i(t)$  which is a real number, where the condition  $\rho_i(t) < 0$  determines the default of the firm. Given a vector  $\rho(0)$  of initial values of robustness across firms and a vector  $s(t)$  of failure states, the robustness of firm  $i$  at the next time step is computed as

$$\rho_i(t+1) = \rho_i^0 - \frac{a}{k_i^{\text{in}}} \sum_{j \in \text{nb}_{\text{in}}(i,A)} s_j(t) \quad (7)$$

with  $\text{nb}_{\text{in}}(i, A)$  being the set of in-neighbors of  $i$ ,  $k_i^{\text{in}}$  the in-degree of  $i$ , and  $a$  a parameter measuring the intensity of the damage caused by the failure. New vectors of failing state vectors and robustness are then computed iteratively until no new failures occur. Mathematically, this process is equivalent to our inward variant model specified by Eqn. (6). The equivalence is obtained by defining fragility  $\phi_i$  as in Eqn. (6) and by setting

$$\theta_i = \frac{\rho_i^0}{a} \quad (8)$$

We note that the model specified in [3] also includes a dynamics on the robustness inbetween two cascades of failures, which is not part of our framework.

Let us now turn to the outward variant of the constant load model. It can be described within our framework by defining fragility as

$$\phi_i(t) = \sum_{j \in \text{nb}_{\text{in}}(i,A)} \frac{s_j(t)}{k_j^{\text{out}}} \quad (9)$$

with  $k_j^{\text{out}}$  being the out-degree of node  $j$ . If the network is undirected and regular, i.e., all nodes have the same degree, the inward and the outward model variants (6), (9) are equivalent and lead to identical dynamics. However, if the degree is heterogeneous, then the number and the identity of the nodes involved in the cascade differ, as shown in the example of Figure 2.

Notice that the influence of high and low out-degree nodes interchange in the two variants, as well as the vulnerability of high and low in-degree nodes. In the inward variant, high in-degree nodes are more protected from contagion as they only fail when many neighbours have failed. In turn, when a high out-degree node fails, it causes a big damage if it has many neighbors with low in-degree. In contrast, in the outward variant, a failing low out-degree node generates a larger impact on its neighbours since the load is distributed among fewer nodes. Thus, a high in-degree node is more exposed to contagion if it is connected to low out-degree nodes. On the other hand, a failing high out-degree node does not cause much damage to its neighbors because the damage gets divided between many nodes. In the examples reported in the figures, the network is undirected and in-degree and out-degree coincide. Still the roles of high-degree and low-degree nodes interchange as discussed above.

As another important difference between the two variants, the maximal fragility is bounded by the value one in the inward variant, while it is bounded by the number of nodes  $n$  in the outward variant, which is realized in a star network. Further, both variants strongly differ regarding the impact of the position of the initial failure. Figure 13 (in Appendix B) shows an example, where node **I** initially fails (instead of node **C** in Figure 2). The cascade triggered by that event is larger in the outward variant than in the inward variant, in contrast to what seen in Figure 2. Eventually, Figure 14 illustrates the dynamics of a cascade triggered by the failure of node **E**, which has the highest degree. This results in a full cascade in the inward variant, while there is no cascade at all in the outward variant. This observation illustrates the different influence of nodes with high degree in the inward and the outward variant, as explained above.

### 3.2 Models with Load Redistribution

Model class (ii) ‘load redistribution’ is our second class of cascading models. In this class all nodes are initially subject to a certain amount of load. Actually, in this model class fragility coincides with load. When a node  $i$  fails, all of its load is redistributed among the first neighbours. This mechanism differs from class (i) because in class (ii) the increase in fragility among the neighbours



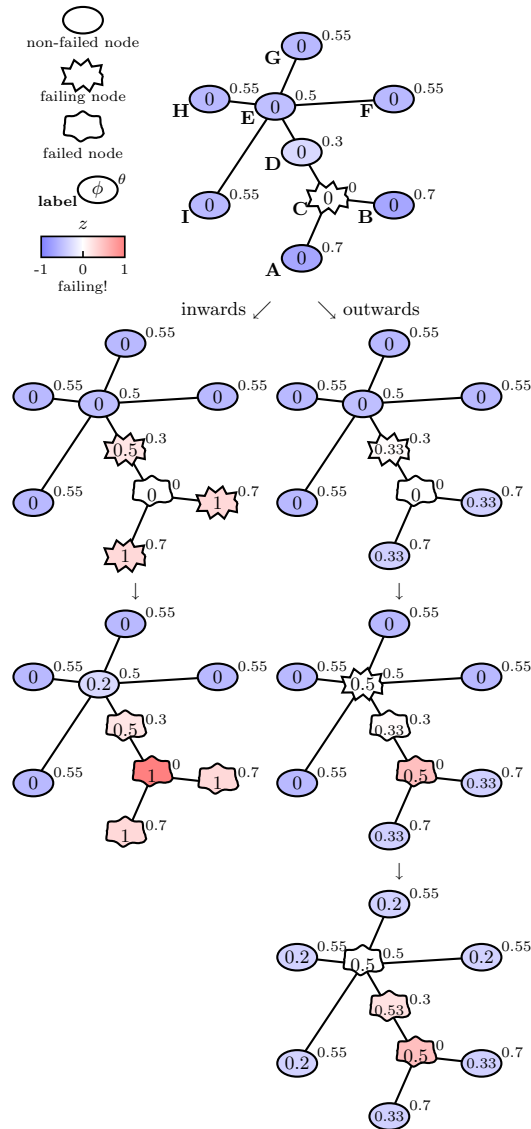


Figure 2: Illustration of the cascading dynamics for the inward (left) and outward (right) variants of model class (i) ‘constant load’, based on the general example of Figure 1. Initially, node C is forced to failure by setting its failure threshold to zero. Subsequent time steps in the evolution of the cascade are represented downward in the figure.

of  $i$  depends on the actual value of  $i$ ’s fragility and not just on the fact that it exceeds the threshold. The damage caused by one failure can thus not be specified a priori.

Models belonging to this class include the fiber bundle model (FBM) [21] and models of cascades in power grids [19]. In some cases it is possible to define the total load of the system, which, additionally, but not necessarily, may be a conserved quantity. For instance, in the FBM a constant force is applied to a bundle of fibers each of which is characterized by a breaking threshold. When a fiber breaks, the load it carries is redistributed equally to all the remaining fibers, so the total load is conserved by definition. In the context of networks, a node represents a fiber and if the node fails the load is transferred locally to the first neighbours in the network. An analogy to power grids is also possible, with nodes representing power plants, links representing transmission lines, fragility representing demand and threshold representing capacity, respectively.

There are, several ways to specify the mechanism of local load transfer. A first variant is the FBM with local load sharing (LLS) and load conservation, investigated in [18]. We refer to this variant as LLSC. Despite the fact that load sharing is local, total load is strictly conserved at any time, due to the condition that links to failed nodes remain able to transfer load (in other words, links do not fail). A second variant implies load shedding instead, and we refer to it as LLSS. In this variant, all links to failed nodes are removed and the load of a failing node is transferred only to the first neighbours that are not about to fail. These are the nodes that are healthy and below the threshold and thus will be still alive at the next time (although they may reach the threshold meanwhile). However, if there are no surviving neighbours, the load is eventually lost (or shed).

In the first variant we can cast the FBM-LLS [18] and extend it to the case of heterogeneous load and directed networks.

From now on, we interpret ‘load’ as ‘fragility’, and ‘capacity’ as ‘failing threshold’. Let  $\phi^0 \in \mathbb{R}^n$  be the vector of initial fragility (corresponding to the initial load carried by each node), and  $\theta$  the vector of failing thresholds (or maximal capacity). (For comparison: In [18] the threshold  $\theta_i$  for node  $i$  is denoted by  $\sigma_i^{\text{th}}$  with values taken from a uniform distribution between zero and one. The load of each node is the same and called  $\bar{\sigma} = \frac{\sigma}{n}$ , with  $\sigma$  being the total load.)

We define

$$\text{reach}_{\text{out}}^{1 \rightarrow 0}(i, s, A) = \{j \mid s_j = 0, \exists \text{ path of 1-nodes } i \rightarrow j\} \quad (10)$$

as the set of healthy nodes which are reachable from node  $i$  following directed paths consisting only of failed nodes (except  $i$ ). Let  $k_i^{\text{reach}_{\text{out}}}$  be the cardinality of such set. Moreover, we define

$$\text{reach}_{\text{in}}^{0 \rightarrow 1}(i, A, s) = \{j \mid s_j = 1, \exists \text{ path of 1-nodes } i \rightarrow j\} \quad (11)$$

to be the set of nodes from which node  $i$  can be reached along directed paths consisting of failed nodes (except  $i$ ). Both sets of nodes defined above have to be computed dynamically based on the current vector of failing states  $s$  and the network.

Finally, given the initial fragility vector  $\phi^0$ , the failure state vector  $s(t)$ , and the network  $A$ , we define the fragility of node  $i$  at time  $t$  in the LLSC variant as

$$\phi_i(t) = \phi_i^0 + \sum_{j \in \text{reach}_{\text{in}}^{0 \rightarrow 1}(i, A, s)} \frac{\phi_j^0}{\#\text{reach}_{\text{out}}^{1 \rightarrow 0}(j, s, A)}. \quad (12)$$

We add that for an undirected network and uniform initial load, such a definition becomes equivalent to the *load concentration* factor of node  $i$ , as defined in [18].

The assumption that links do not break and remain able to transfer load is not always satisfactory. Some models have thus investigated the LLSS variant of the model in which the load is transferred only to the surviving first neighbours [23]. In this case the load transfer is truly local and there is no transmission along a chain of failed nodes. This implies that during a cascade of failures, at some point in time the network might split into disconnected components which cannot transfer load to each other. In particular, if one of these subnetworks fails entirely, all the load carried by this subnetwork is shed.

As a consequence of the LLSS assumption, fragility now is not just a function of the current state vector  $s(t)$  and some static parameters (such as the network matrix and the initial fragility  $\phi^0$ ). In contrast, it has to be defined through a dynamic process as a function of the fragility vector at previous time  $t$ , according to the following equation:

$$\phi_i(t+1) = \begin{cases} \phi_i(t) + \sum_{j \in \text{fail}_{\text{in}}(i)} \frac{\phi_j(t)}{\#\text{hea}_{\text{out}}(j)} & \text{if } \begin{cases} s_i(t) = 0, \\ \phi_i(t) < \theta_i \end{cases} \\ 0 & \text{otherwise,} \end{cases} \quad (13)$$

with  $\text{fail}_{\text{in}}(i)$  being the set of in-neighbors of  $i$  which fail at time  $t$  (but have not already failed!), and  $\text{hea}_{\text{out}}(j)$  the set of out-neighbors of  $j$  which remain healthy at time  $t+1$

$$\begin{aligned} \text{fail}_{\text{in}}(i) &= \{j \mid j \in \text{nb}_{\text{in}}(i, A), s_j(t) = 0, \phi_j(t) \geq \theta_j\}, \\ \text{hea}_{\text{out}}(j) &= \{i \mid i \in \text{nb}_{\text{out}}(j, A), s_i(t) = 0, \phi_i(t) < \theta_i\}. \end{aligned} \quad (14)$$

Thus, Eqn. (13) is well defined unless  $\text{hea}_{\text{out}}(j)$  is empty. In this case, there is no healthy neighbour of  $j$  to which the load can be transferred, thus the load has to be shed. The remaining healthy nodes remain unaffected.

Figure 3 illustrates, as an example, the different outcomes of the dynamics in the LLSC and LLSS variants. The initial load is set to one for all nodes, thus the total load on the system is nine. The values of the threshold are set in order to have the same values of  $z = \phi - \theta$  at each node as in the example of Figure 1. As in Figure 2, we set the failing threshold of node **C** to one in order to trigger an initial failure.

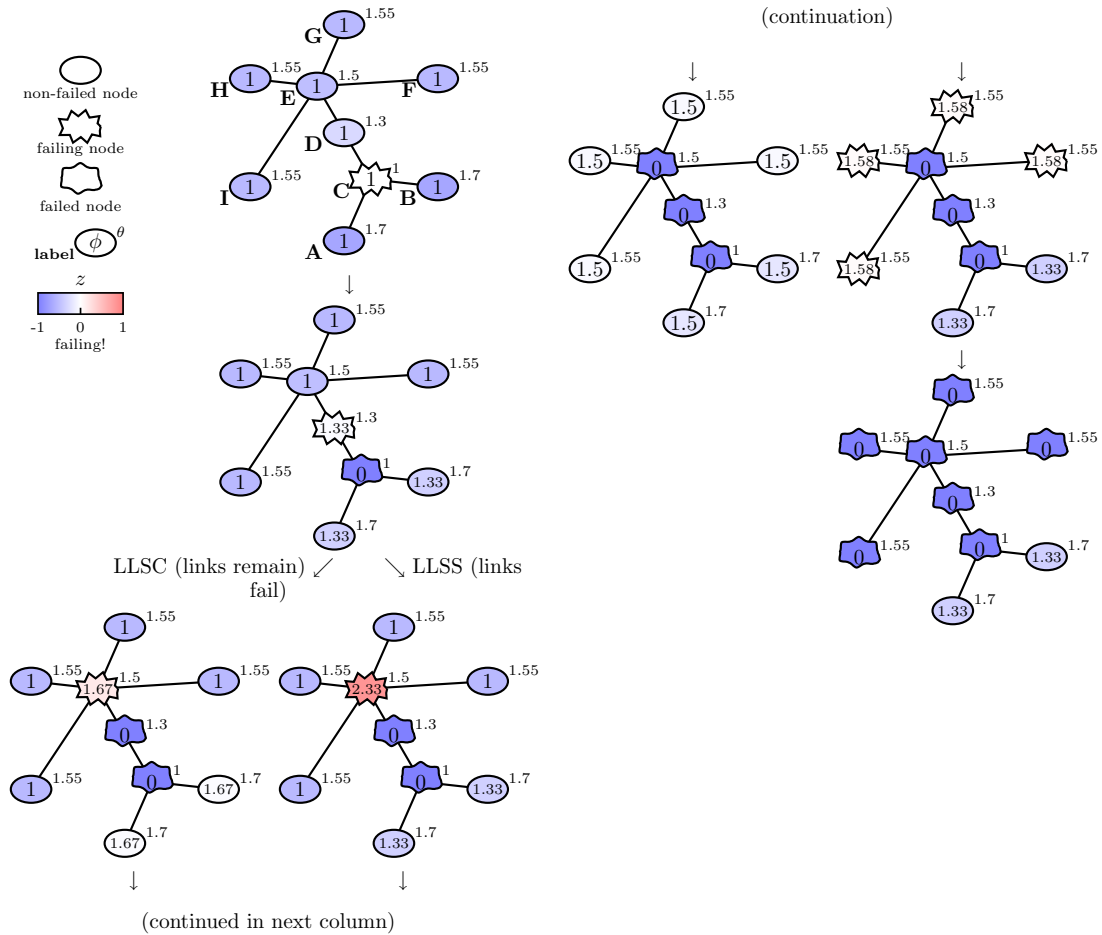


Figure 3: Illustration of the cascading dynamics for the two variants of the model class (ii) ‘load redistribution’, based on the general example in Figure 1. Left: LLSC variant, following Eqn. (12). Right: LLSS variant following Eqn. (13). Again, initially node C is forced to failure. The dynamics is the same for the two variants in the first time step but it differs in the subsequent time steps.

On one hand, we could expect that cascades triggered by the failure of one node are systematically wider in the LLSC variant than in the LLSS variant because in the first one the total load is conserved. On the other hand, in the LLSC, the fragility is redistributed also to indirect neighbours thus leading to a smaller increase of fragility per node and therefore possibly to smaller cascades. In fact there seems to be no apparent systematic result, the outcome being dependent on the network structure and the position of the initial failure. In the example shown in Figure 3 the cascade stops sooner in the LLSC variant than in the LLSS one, due to the

rebalancing of load across the network. In other cases, however, if for instance node **E** initially fails, we find that the load shedding has a stronger impact and the cascade is smaller in the LLSS case.

### 3.3 Models with Overload Redistribution

We conclude our classification with class (iii) ‘overload redistribution’. When a node  $i$  fails in these models, only the difference between the load and the capacity is redistributed among the first neighbours. Actually, the overload of a node is its net fragility. This class is more realistic in applications, where a failed node can still hold its maximum load and only has to redistribute its overload.

The Eisenberg-Noe model is an important example of an economic model in which firms are connected via a network of liabilities [12]. When the total liabilities of a firm  $i$  exceed its expected total cash flow (consisting of the operating cash flow from external sources and the liabilities of the other firms towards  $i$ ), the firm goes bankrupt. When a new bankruptcy is recognized the expected payments from others decline, but they do not vanish entirely. Thus the loss spreading to the creditors is mitigated.

With respect to our framework, we can identify the total liability minus the currently expected payments (from the liabilities of others) with fragility. Similarly, operating cash flow corresponds to the failing threshold. The relation between the Eisenberg-Noe model and the overload redistribution class is discussed more in detail in Appendix A.

Therefore, we adapt the two variants of load redistribution defined as LLSC and LLSS in Section 3.2 to the case of overload redistribution by subtracting the threshold value in the nominator of Eqns. 12 and 13. We have

$$\phi_i(t) = \phi_i^0 + \sum_{j \in \text{reach}_{\text{in}}^{0 \rightarrow 1}(i, A, s)} \frac{\phi_j^0 - \theta_j}{\#\text{reach}_{\text{out}}^{1 \rightarrow 0}(j, s, A)}. \quad (15)$$

as definition of fragility in the LLSC version when links remain, and

$$\phi_i(t+1) = \begin{cases} \phi_i(t) + \sum_{j \in \text{fail}_{\text{in}}(i)} \frac{\phi_j(t) - \theta_j}{\#\text{hea}_{\text{out}}(j)} & \text{if } \begin{matrix} s_i(t) = 0, \\ \phi_i(t) < \theta_i \end{matrix} \\ 0 & \text{otherwise,} \end{cases} \quad (16)$$

as dynamical equation of fragility in the LLSS version when links break.

Using our small example of Figure 1, the cascading dynamics for the model class (iii) is presented in Figure 4. In general, as we will see in Section 4 this class of models leads to much smaller cascades, compared to class (ii). In this example, we have set the initial fragility of node **C** high

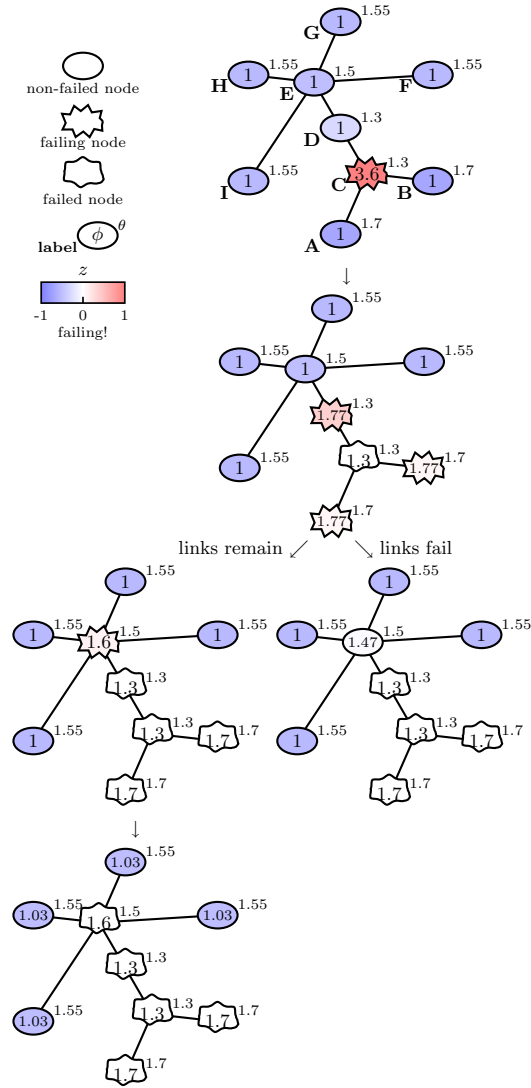


Figure 4: Illustration of the cascading dynamics for model class (iii) ‘overload redistribution’. Left: LLSC variant based on Eqn. (15). Right: LLSS variant based on Eqn. (16).

enough so that a large cascade is triggered. A very high initial overload is needed to trigger a cascade of failures because this overload is the only amount which is transferred through the whole system. On a failure nothing new is added to the total amount, because the node stays with its maximum capacity.

Notice that the models of overload redistribution are invariant to joint shifts in the initial fragility

$\phi^0$  and in the failing threshold  $\theta$ . In other words, a system with  $\phi^0 + c$  and  $\theta + c$  leads to the same trajectory of failure state  $s(t)$  and fragility  $\phi(t) + c$ . Thus, it is enough to study the model with  $\phi^0 = 0$  without loss of generality.

## 4 Macroscopic reformulations

In the previous section we have seen that the different classes of cascading models lead to a diverse behaviour, at least in small scale examples, even if initial conditions for net fragility are the same. In this section, by studying simple mean-field approximations of the processes we find that there are significant differences also at the macroscopic level. In order to compare the different model classes under the same conditions, we have set the probability density functions  $p_{z(0)}$  of initial values of the net fragility to be equal for all models. For the cases (i) constant load, and (iii) overload redistribution we set  $\theta = -z(0)$ . Notice, that we can set  $\phi^0 = 0$  in case (iii) without loss of generality. For case (ii) load redistribution, instead, it is necessary to have  $\phi^0 > 0$  (otherwise there is no load to redistribute) and we have  $\theta = \phi^0 - z(0)$ . We further assume that the initial fragility  $\phi^0$  is uniform across nodes in model class (ii).

Even a basic mean-field approach allows for an interesting comparison of the three model classes. To do so, we replace the distribution of fragility at time  $t$ , with the delta function  $\delta_{\langle\phi(t)\rangle}$  centered on the mean fragility  $\langle\phi(t)\rangle$ . This is equivalent to assuming a fully connected network since in such a case Eqns. (6-13) yield the same fragility for every node. If the two distributions are independent, from (5) we get

$$p_{z(t)} = \delta_{\langle\phi(t)\rangle} * p_{-\theta}. \quad (17)$$

Convolution with a delta corresponds to a shift in the variable, so that  $p_{z(t)} = p_{\langle\phi(t)\rangle - \theta}$ , and from Eqn. (3) we obtain

$$\begin{aligned} X(t+1) &= \int_0^\infty p_{\langle\phi(t)\rangle - \theta}(z) dz = \int_{-\langle\phi(t)\rangle}^\infty p_{-\theta}(z) dz \\ &= \int_{-\infty}^{\langle\phi(t)\rangle} p_\theta(z) dz = P_\theta(\langle\phi(t)\rangle) \end{aligned} \quad (18)$$

where  $P_\theta(x) = \int_{-\infty}^x p_\theta(\theta) d\theta$  is the cumulative distribution function of  $\theta$ . This is equivalent to a change of variable  $z(t) = \langle\phi\rangle - \theta$  in the probability distribution and in the integral. However, the procedure with convolution can be carried out also if  $p_\phi$  is not assumed to be a delta function.

At this point, we have to express the mean fragility  $\langle\phi(t)\rangle$  in terms of the current fraction of failed nodes,  $X(t)$ . For case (i) 'constant load', in a fully connected network, Eqns. (6) and (9) yield both the following mean fragility:

$$\langle\phi(t)\rangle = X(t) \quad (19)$$

For case (ii) 'load redistribution', assuming that the surviving nodes equally share the initial load, we can write for the mean fragility:

$$\langle \phi(t) \rangle = \frac{\phi^0}{1 - X(t)} \quad (20)$$

This is obtained from Eqn. 12 at microscopic level by taking the mean over all  $i$  on both sides

$$\langle \phi_i(t) \rangle = \langle \phi_i^0 \rangle + \left\langle \sum_{j \in \text{reach}_{\text{in}}^{0 \rightarrow 1}(i, A, s)} \frac{\phi_j^0}{\#\text{reach}_{\text{out}}^{1 \rightarrow 0}(j, s, A)} \right\rangle \quad (21)$$

Now, assuming  $\phi_i^0 = \phi^0$  for all nodes and the network as fully connected, we have that:  $\langle \phi_i^0 \rangle$  coincides with  $\phi^0$ ; the sum over the set  $\text{reach}_{\text{in}}^{0 \rightarrow 1}(i, A, s)$  (which now coincides with the set of failed nodes) equals  $nX(t)$ ; and  $\#\text{reach}_{\text{out}}^{1 \rightarrow 0}(j, s, A)$  equals  $n(1 - X(t))$ , because we count all healthy nodes. Thus, we obtain

$$\langle \phi(t) \rangle = \phi^0 + \frac{nX(t)\phi^0}{n(1 - X(t))} = \frac{\phi^0}{1 - X(t)}. \quad (22)$$

For case (iii) 'overload redistribution', we can proceed similarly starting from Eqn. 15. Setting  $\phi_i^0 = 0$ , without loss of generality, and taking the mean over  $i$  on both sides yields

$$\langle \phi_i(t) \rangle = \left\langle \sum_{j \in \text{reach}_{\text{in}}^{0 \rightarrow 1}(i, A, s)} \frac{-\theta_j}{\#\text{reach}_{\text{out}}^{1 \rightarrow 0}(j, s, A)} \right\rangle \quad (23)$$

Again, we can replace the sum over  $\text{reach}_{\text{in}}^{0 \rightarrow 1}(i, A, s)$  by  $nX(t)$ , and  $\#\text{reach}_{\text{out}}^{1 \rightarrow 0}(j, s, A)$  by  $n(1 - X(t))$ . However, now the average of the threshold values  $\theta_j$  across all failed nodes (as indicated by the sum) is not simply  $\langle \theta \rangle$ . It is instead the mean of that part of the distribution  $p_\theta$  where failed nodes are located. These are the nodes with  $\theta \leq \phi(t)$  and their probability mass has to sum up to  $X(t)$ . For a given distribution  $p_\theta$  and a given fraction  $X$  of failed nodes, the mean threshold of failed nodes is defined as

$$\langle \theta \rangle_X = \left( \int_{-\infty}^{q_X} \theta p_\theta(\theta) d\theta \right) / X. \quad (24)$$

$q_X$  denotes the  $X$ -quantile of the distribution  $p_\theta$ , i.e. a fraction  $X$  of the probability mass lies below  $q_X$ :

$$X = \int_{-\infty}^{q_X} p_\theta(\theta) d\theta \quad (25)$$

Thus,  $\langle \theta \rangle_X$  is the first moment of  $\theta$  below the value  $q_X$ , normalized by the probability mass of the distribution  $p_\theta$  in the same interval. Replacing this into Eqn. (23) yields as mean fragility for case (iii) overload redistribution:

$$\langle \phi(t) \rangle = \frac{-\langle \theta \rangle_{X(t)} X(t)}{1 - X(t)}. \quad (26)$$



Notice, that the mean of the threshold of the failed nodes is negative, thus the minus in front of  $\langle \theta \rangle_{X(t)}$  ensures that fragility is positive.

By replacing the expressions of  $\langle \phi(t) \rangle$  in terms of  $X(t)$  in Eqn. (18) we obtain simple recursive equations in  $X(t)$  for the different cases: For case (i) 'constant damage'

$$X(t+1) = P_\theta(X(t)), \quad (27)$$

for case (ii) 'load redistribution'

$$X(t+1) = P_\theta \left( \frac{\phi^0}{1 - X(t)} \right), \quad (28)$$

and for case (iii) 'overload redistribution'

$$X(t+1) = P_\theta \left( \frac{-\langle \theta \rangle_{X(t)} X(t)}{1 - X(t)} \right). \quad (29)$$

As the functions on the right hand sides of Eqns. (27)-(29) are monotonic non-decreasing and bounded within  $[0, 1]$ ,  $X(t)$  always converges to a fix point  $X^*$  representing the final fraction of failed nodes.

With these iterations we can study the three different models systematically on the same initial conditions. We assume the failing thresholds to be normally distributed such that  $z(0) \sim \mathcal{N}(-\mu, \sigma)$  in all three cases. This is guaranteed if  $\theta \sim \mathcal{N}(\mu, \sigma)$  for the cases of constant load and overload redistribution, and if  $\theta \sim \mathcal{N}(\mu + \phi^0, \sigma)$  for the case of load redistribution. The parameters  $\mu$  and  $\sigma$  represent the mean and the standard deviation of the net fragility. Particularly,  $\sigma$  represents the initial heterogeneity across agents. The initial fraction of failed nodes is thus  $X(0) = \Phi_{\mu, \sigma}(0)$  where  $\Phi_{\mu, \sigma}$  denotes the cumulative distribution function of a normal distribution with mean  $\mu$  and standard deviation  $\sigma$ . The surface of values taken by the initial fraction of failed nodes  $X(0)$  over the plane  $(\mu, \sigma)$  is shown in Figure 5. This is assumed to be the same in all three cases.

In contrast, the final fraction of failed nodes,  $X^*$ , obtained as numerical solution of the recursive equations (27)-(29) is shown in Figure 6. Moreover, the difference between the two previous quantities,  $X^* - X(0)$ , representing the fraction of nodes which fail due to the cascade process, is shown in Figure 7.

At the macro level, the most important structural difference between the three model classes concerns the existence of a discontinuity and its boundaries in the landscape of  $X^*$ . Since  $X^*$  can be considered an order parameter for our system, regions with different values separated by a discontinuity indicate a first-order phase transition. The proximity of the discontinuity, i.e. across the boundary of the phase transition, marks a region of great interest from the point of

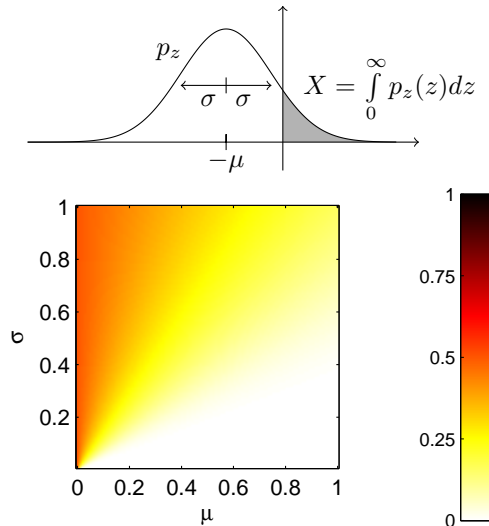


Figure 5: Top: Illustration of the distribution of net fragility and geometric interpretation of  $X$ . Bottom: Initial fraction of failing nodes  $X(0)$  as a function of mean  $-\mu$  and standard deviation  $\sigma$  of the distribution of initial net fragility  $z(0) = \phi(0) - \theta$ . The distribution is assumed to be normal.

view of systemic risk. Indeed a small change in the distribution of initial net fragility can mean the difference between a negligible cascade or a full breakdown. In the case of 'constant load', we find a discontinuity between a region with low systemic risk and one with high systemic risk, with a separation line that starts at  $(\mu, \sigma) = (0, 0)$  and monotonically increases in  $\mu$  and  $\sigma$ . However, above  $(\mu, \sigma) \approx (0.5, 0.4)$  the discontinuity vanishes. In the case of load redistribution, instead, the a region of full break down is always separated by a discontinuity from the region of partial survival. Interestingly, the separation line when  $\mu$  is seen as a function of  $\sigma$  is not monotonic. For some  $\mu$  (e.g  $\mu = 0.2$  when  $\phi^0 = 0.25$ ) most nodes survive for small  $\sigma$ , half of the nodes survive for large  $\sigma$  but all nodes fail for intermediate  $\sigma$ . This means that the system is more robust for low heterogeneity and high heterogeneity, but more susceptible to systemic risk in the region of intermediate heterogeneity. Finally, in the case of overload redistribution region of full breakdown is reduced to the line with  $\mu = 0$  with no discontinuity towards the region of partial survival.

Figure 8 shows the difference in the final fraction of failed nodes between the different model classes. For instance, the top left plot shows the difference between class (i) and (ii),  $X_{(i)}^* - X_{(ii)}^*$ . It indicates that constant load implies larger fraction of failures than load redistribution, when the initial load is small ( $\phi^0 = 0.25$ ). This, however, does not hold for small  $\mu$  and large  $\sigma$ , where more nodes survive with constant load. Overload redistribution leads to smaller systemic

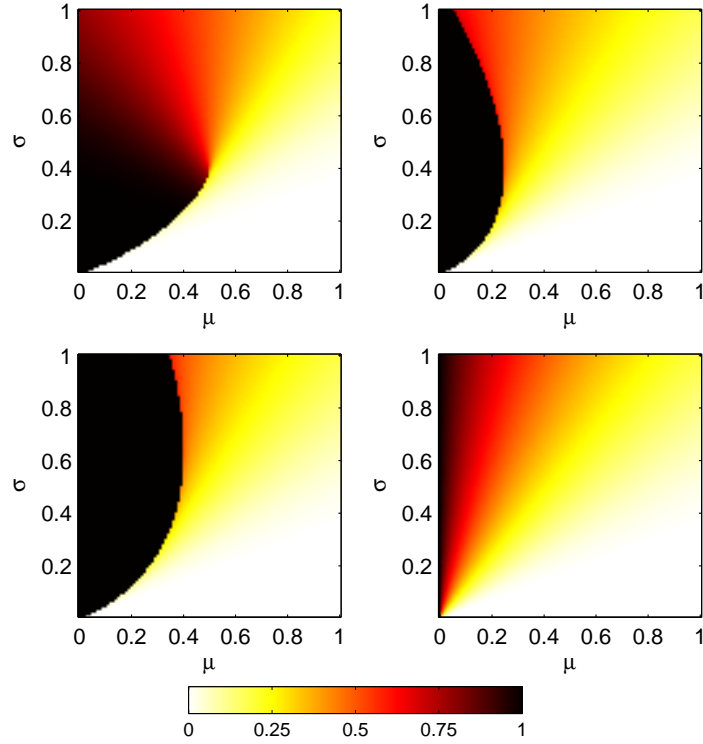


Figure 6: Final fraction of failed nodes  $X^*$  in mean field approximation. As shown in Fig. 5, the values  $-\mu$  and  $\sigma$  refer to the initial distribution of  $z(0) = \phi(0) - \theta$ . The various plots refer to the different model classes. Top left: class (i) constant load. Top right: class (ii) load redistribution with initial load  $\phi^0 = 0.25$ . Bottom left: class (ii) with  $\phi^0 = 0.4$ . Bottom right: class (iii) overload redistribution.

risk than constant load (top right part of Figure 8) and load redistribution (bottom left part of Figure 8), except for very high  $\mu$  and small  $\sigma$ . Interestingly, there is no model class which leads to smaller systemic risk in the whole  $(\mu, \sigma)$ -plane than the others. Finally, the parameter  $\phi^0$  in the load redistribution model has a monotonic effect: The larger it is the larger is the systemic risk (bottom right part of Figure 8).

Even under the basic assumption of a fully connected network, the analysis carried out so far (denoted in the following as MF1) was able to provide some insights in the relations among the three model classes. The following remark is in order at this point. Mean field approaches have known limitations. In principle, the foregoing analysis has little to say about the outcome of individual realizations. For instance, consider the top right corner of the top left plot of Fig. 6. In that region,  $X^*$  takes intermediate values around 0.25. Does this imply that one time every four there is a full breakdown and otherwise no failure? Or, does it imply that in every realization one

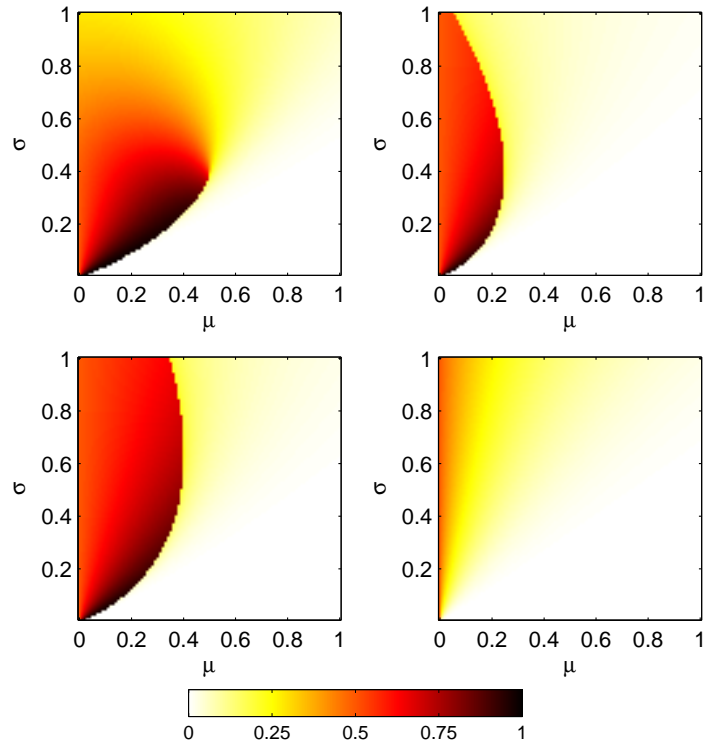


Figure 7: Net fraction of failed nodes  $X^* - X(0)$  due to the cascading process. Plots are obtained from those in Figure 6 by subtracting the initial number of failed nodes (shown in Figure 5).

fourth of the nodes fail? Notice that the cascade process is deterministic, and that the sources of variability that are relevant for our purposes are the initial distribution of net fragility  $z(0)$  and the network structure  $A$ . Our simulations show that, in absence of strong correlation in  $z(0)$  across nodes and in absence of strong modularity in the network, the variability of  $X^*$  across realizations is quite limited. A robustness analysis is left as future work. For sure, in the regions in which  $X^*$  is very close to 1 the variability across realization is negligible and this is a useful result in terms of systemic risk estimation. Finally, a strong variability is expected, as usual, in the proximity of the transition between small and large systemic risk.

The mean-field approach, could now be refined in various ways, in order to take into account, for instance, the cases of non-fully connected network, heterogeneous degree, or even degree-degree correlation, following the methods that have been applied to epidemic spreading models [26, 5]. These investigation are left as future work.

In the remainder of this section, as an example, we analyse further the constant load class on

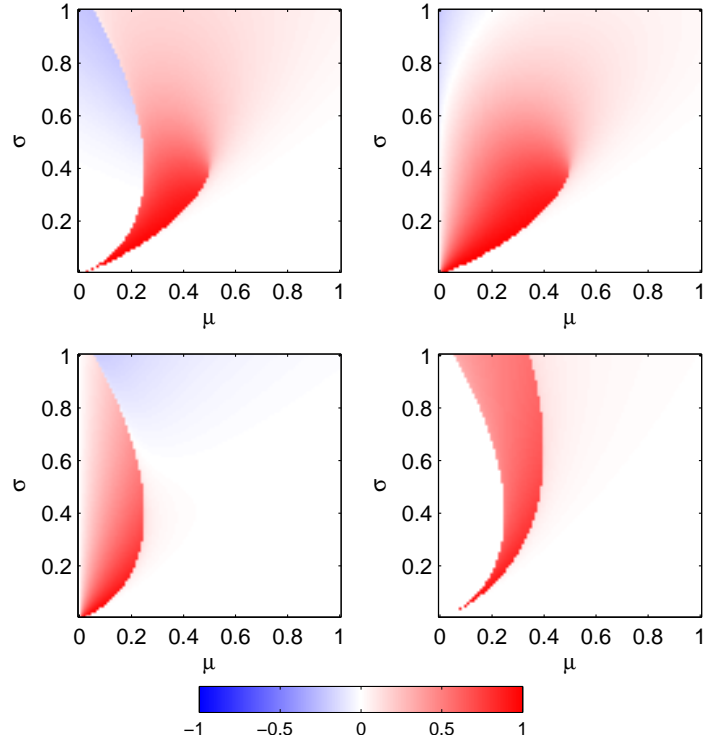


Figure 8: Difference in fraction of failed nodes between class models. Top Left:  $X_{(i)}^* - X_{(ii)}^*$ . Top Right:  $X_{(i)}^* - X_{(iii)}^*$ . Bottom Left:  $X_{(ii)\phi^0=0.25}^* - X_{(iii)}^*$ . Bottom Right:  $X_{(ii)\phi^0=0.4}^* - X_{(ii)\phi^0=0.25}^*$ .

a network in which each node has on average  $k$  neighbors (instead of  $n - 1$ ). This provides a first step to address the influence of network topology on systemic risk. The fragility of a node now takes values in the discrete set  $\{0, 1/k, 2/k, \dots, j/k, \dots, 1\}$ . The probability of each event corresponds to the probability that  $j$  out of  $k$  neighbours fail at the same time, given that each fails with probability  $q$ . If failures among neighbours of a node are independent, such probability follows a binomial distribution  $B(j, k, q)$ . We can further approximate the probability  $q$  that a node fails with the total fraction of failed nodes  $X$ . Thus, we can write the probability density function for the fragility as follows

$$p_{\phi(t)} = \sum_{j=0}^k B(j, k, X(t)) \delta_{\frac{j}{k}}$$

with  $B(j, k, X) = \binom{j}{k} X^j (1 - X)^{k-j}$ . (30)

It follows

$$\begin{aligned}
p_{z(t)} &= \left( \sum_{j=0}^k B(j, k, X(t)) \delta_{\frac{j}{k}} \right) * p_{-\theta} \\
&= \sum_{j=0}^k B(j, k, X(t)) p_{-\theta + \frac{j}{k}}
\end{aligned} \tag{31}$$

from which we can derive recursive equations in  $X(t)$  analogous to Eqns. (27)–(29), to compute  $X^*$ . A similar approach is used also in [11]. We denote this approach with MF2.

We can further refine the analysis by formulating a recursive equation for the whole distribution  $p_{z(t)}$  rather than for  $X(t)$ . This approach can then take into account the fact that the distribution of  $z(t)$  is reshaped (and not simply shifted) during the dynamics.

For this purpose, we define the partial pdf of healthy nodes  $p_{z(t)}^h = \mathbf{1}_{[-\infty, 0]} p_{z(t)}$ , where  $\mathbf{1}_{[a, b]}$  takes value one on the interval  $[a, b]$  and zero elsewhere. The integral of this function over the whole real axis gives the fraction of healthy nodes, while the fraction of failed nodes is given by

$$X(t) = 1 - \int_{-\infty}^0 p_{z(t)}^h dz. \tag{32}$$

Notice that the total mass of the function  $p_{z(t)}^h$  is in general smaller than one and decreases over time (therefore, strictly speaking  $p_{z(t)}^h$  is not a pdf). Because  $p_{z(t)}^h$  only counts the healthy nodes, the *fraction of currently failing* (and not already failed!) nodes,  $X_f$ , is defined as

$$X_f(t) = \int_0^{\infty} p_{z(t)}^h(z) dz \tag{33}$$

We can then write the recursive equation

$$\begin{aligned}
p_{z(t+1)}^h &= \left( \sum_{j=0}^k B(j, k, X_f(t)) \delta_{\frac{j}{k}} \right) * (\mathbf{1}_{[-\infty, 0]} p_{z(t)}^h) \\
&= \sum_{i=0}^k B(j, k, X_f(t)) \mathbf{1}_{[-\infty, \frac{i}{k}]} p_{z(t) + \frac{i}{k}}^h.
\end{aligned} \tag{34}$$

Summarizing, from Eqn. (34) we can solve for the limit distribution  $p_z^{h*}$  or compute it numerically (after binning the  $z$ -axis). This last method is denoted as MF3.

Methods MF2 and MF3 can be understood as conceptually different by focussing on the net fragility of a single node coming for the distribution. For MF2 we compute the probability of a node to have a certain net fragility by its possibilities to have  $0, 1, 2, \dots, k$  failed neighbors, thus

the maximum increase in fragility is  $\frac{k}{k}$  over all time steps. This fits to the inward agent-based dynamics, because we focus on the receiving node which has  $k$  in-neighbors. In MF3 instead, after each time step the whole distribution of the net fragility is reshaped. Thus, there is a nonzero probability that one node gets more than  $k$  increases in net fragility in successive time steps. We compute how the fraction of currently failing nodes reshapes the distribution of net fragility. Thus, we focus on the spreading node here and there is a nonzero probability that one node can receive more than  $k$  increases of  $\frac{1}{k}$  in two successive time steps, as it is also possible in a network where in-degrees vary slightly. Thus, MF3 fits to the outwards agent-based dynamics.

Figures 9, 10, and 11 plot the limit fraction  $X^*$  of failed nodes in the  $(\mu, \sigma)$  plane obtained from the recursive Equations (31) (MF2) and (34) (MF3), as well as a comparison with the case of fully connected network (MF1) and a comparison between each other. Notice that, similar to MF1, we still observe in both MF2 and MF3 a discontinuity line which vanishes as  $\mu$  and  $\sigma$  increase. The shape of the line varies in the three analyses. In the third approach, MF3, the values of  $X^*$  are systematically smaller than in MF2.

Moreover, in MF1 the region of high systemic risk is less extended than in the other approaches, although for intermediate values of  $\mu, \sigma$ , values of  $X^*$  in MF1 are larger than in MF2, MF3 (blue regions in Fig. 11). This is due to the fact that when many links are present, nodes are spreading the fragility more evenly and so less failures take place, given the same initial fragility. After the critical point the avalanche is larger.

On the other hand, approach MF2 always yields larger systemic risk than MF3 which takes into account the whole distribution (see Fig. 11). Thus, the inwards version of the ‘constant load’ model is more prone to systemic risk than the outward version, this is especially relevant in the region of very low  $\sigma$ , where MF2 shows full cascades up to  $\mu \approx 0.3$ , while MF3 is already free from full cascades. A full cascade in MF3 is triggered only for slightly higher  $\sigma$ .

## 5 Generalization to Stochastic Cascading Models

### 5.1 Stochastic description

In Section 2 we have introduced a general model of cascades based on a deterministic dynamics of the state  $s_i(t)$  of a node  $i$ , Eqn.( 2), with a sharp transition from healthy to failed state, at exactly  $z_i = 0$ . In this Section we propose a generalization of such process to a stochastic setting. Interestingly, it will be possible to derive the Voter Model as well as the stochastic contagion model SIS as particular cases. This exercise will shed some new light on the connections between cascade models and contagion models.

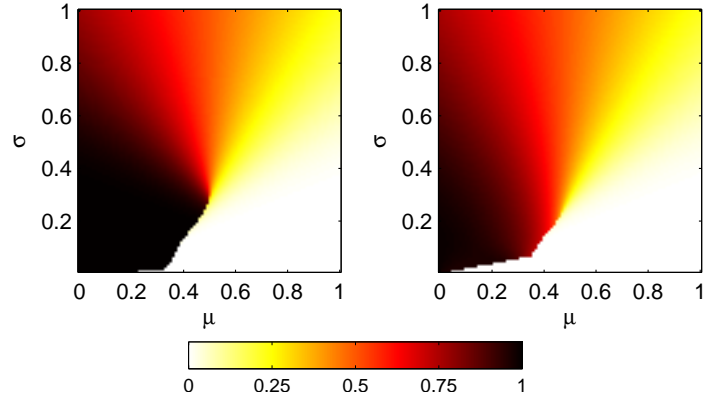


Figure 9: Model class (i) 'constant damage', fraction of failed nodes  $X^*$  on a regular graph with degree  $k = 3$ . Plots are constructed in analogy to Figure 6. Left: mean field solution from Eqn. (31) (MF2). Right: mean field solution from Eqn. (34)(MF3).

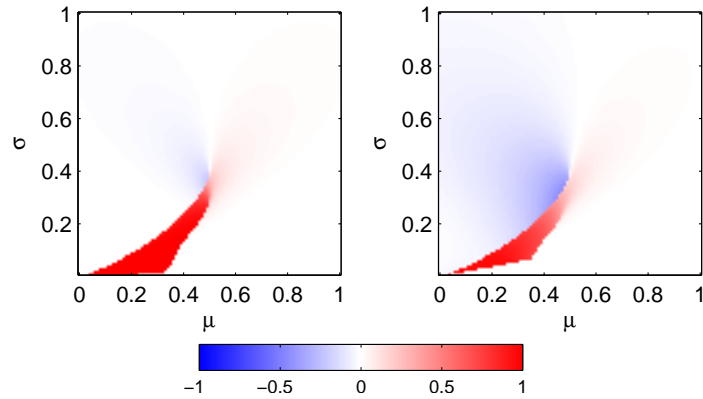


Figure 10: Model class (i) 'constant damage'. Difference between fraction of failed nodes  $X^*$  on a regular graph with degree  $k = 3$  (shown in Figure 9) and on a fully connected network (shown in Figure 6), based on different mean field approaches. Left: plot of the difference  $X_{MF2}^* - X_{MF1}^*$ . Right:  $X_{MF3}^* - X_{MF1}^*$ . Color code as in Fig. 8. .

We assume that the failure of a node  $i$  is a stochastic event occurring with some probability dependent on the net fragility,  $z_i(t)$ , but possibly also conditional to the current state,  $s_i(t)$ . We have in mind a situation in which the probability to fail increases monotonically as  $z_i(t) = \phi_i - \theta_i$  becomes positive. Conversely, nodes can switch from the failed state back to the healthy state and this is more likely if  $z_i(t) = \phi_i - \theta_i$  becomes negative. Notice that we introduce an asymmetry,



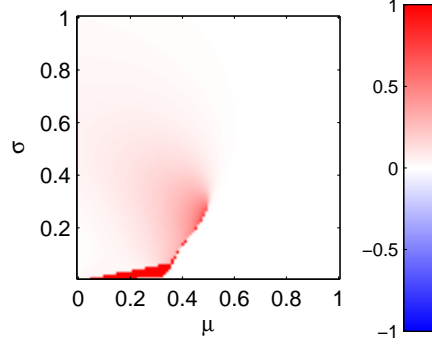


Figure 11: Model class (i) 'constant damage'. Difference  $X_{\text{MF2}}^* - X_{\text{MF3}}^*$  between final fraction of failed nodes obtained with approaches MF2 and MF3 shown in Figure 9. Color code as in Fig. 8.

as  $\theta'_i \neq \theta_i$  in general. Compared to Equation (2), now the dynamics is defined as

$$s_i(t+1) = \begin{cases} 1 & \text{with } p_i(1, t+1|1, t; z_i) & \text{if } s_i(t) = 1 \\ 1 & \text{with } p_i(1, t+1|0, t; z_i) & \text{if } s_i(t) = 0 \\ 0 & \text{with } p_i(0, t+1|0, t; z'_i) & \text{if } s_i(t) = 0 \\ 0 & \text{with } p_i(0, t+1|1, t; z'_i) & \text{if } s_i(t) = 1 \end{cases} \quad (35)$$

Here,  $p_i(1, t+1|0, t; z_i)$  denotes the probability to find node  $i$  in state 1 at time  $t+1$ , conditional that it was in state 0 at time  $t$ , etc. Obviously,

$$\begin{aligned} 1 &= p_i(1, t+1|1, t; z_i) + p_i(0, t+1|1, t; z'_i) \\ 1 &= p_i(0, t+1|0, t; z'_i) + p_i(1, t+1|0, t; z_i) \end{aligned} \quad (36)$$

In the following, we abbreviate the relevant conditional probabilities as  $p(1|0, z_i) = p_i(1, t+1|0, t; z_i)$ ,  $p(0|1; z'_i) = p_i(0, t+1|1, t; z'_i)$  and denote them as transition probabilities (per unit of time). Under Markov assumptions the Chapman-Kolmogorov equation holds for the probability to find node  $i$  in state 1 at time  $t+1$ :

$$\begin{aligned} p_i(1, t+1) &= p_i(1, t+1|1, t; z_i) p_i(1, t) \\ &\quad + p_i(1, t+1|0, t; z_i) p_i(0, t) \end{aligned} \quad (37)$$

With

$$1 = p_i(1, t) + p_i(0, t) \quad (38)$$

and Eqn. (36), this results in the dynamic equation

$$\begin{aligned} p_i(1, t+1) - p_i(1, t) &= -p(0|1; z'_i) p_i(1, t) \\ &\quad + p(1|0, z_i) [1 - p_i(1, t)] \end{aligned} \quad (39)$$

Stationarity, i.e.  $p_i(1, t + 1) - p_i(1, t) = 0$ , implies the so-called detailed balance condition:

$$\frac{p_i(1)}{1 - p_i(1)} = \frac{p(1|0; z'_i)}{p(0|1; z_i)} \quad (40)$$

A very common assumption for  $p_i(1)$  is the logit function:

$$p_i(1; \beta, \beta'; z_i, z'_i) = \frac{\exp(\beta z_i)}{\exp(\beta z_i) + \exp(-\beta' z'_i)} \quad (41)$$

The parameters  $\beta, \beta'$  measure the impact of stochastic influences on the transition into the failed state and back into the healthy state, accordingly. By varying  $\beta, \beta'$  the deterministic case ( $\beta, \beta' \rightarrow \infty$ ) as well as the random case ( $\beta, \beta' \rightarrow 0$ ) can be covered. Figure 12 shows the dependency of the probability  $p = p(1)$  with respect to  $\beta$  for the symmetric case,  $\beta = \beta', z = z_i = z'_i$ .

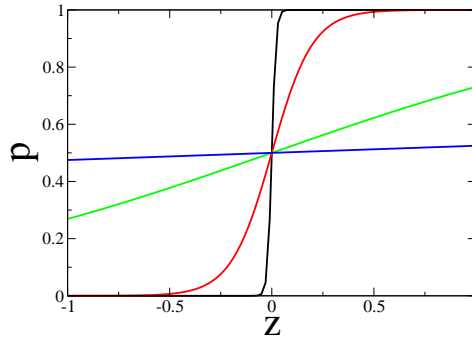


Figure 12: Probability  $p = p(1)$ , eqn. (41), dependent on  $z = z_i = z'_i$  for several values of  $\beta = \beta'$ , to indicate the crossover from a random to a deterministic transition: (blue)  $\beta = 0.05$ , (green)  $\beta = 0.5$ , (red)  $\beta = 5$ , (black)  $\beta = 50$

The transition probabilities can be chosen in accordance with Eqs. (40), (41) as follows:

$$\begin{aligned} p(1|0; z_i) &= \gamma \frac{\exp(\beta z_i)}{\exp(\beta z_i) + \exp(-\beta' z'_i)} \\ p(0|1; z'_i) &= \gamma' \frac{\exp(-\beta' z'_i)}{\exp(\beta z_i) + \exp(-\beta' z'_i)} \end{aligned} \quad (42)$$

The parameters  $\gamma, \gamma'$  set the range of the functions and should be equal only if the detailed balance condition holds. The different thresholds  $\theta, \theta'$  shift the position of the transition from one state to the other. The transition probabilities thus depend on two sets of parameters,  $\gamma, \beta, \theta$  characterizing the transition into the failed state, and  $\gamma', \beta', \theta'$  for the transition into the healthy state. These sets differ in principle, but they play the same role in the transitions.

## 5.2 Mean-field equations

In analogy to Section 4, we want to derive a dynamics at the macro level for the expected fraction  $X(t)$  of failed nodes at time  $t$ . To this end, we start from the micro dynamics given by Eqn. (39). As a first mean-field assumption, we neglect correlations between fragility and thresholds across nodes in the network. In other words, we assume that the values of  $z_i$  and  $z'_i$  are drawn from the same probability distribution  $p_z(z(t))$ , regardless of the identity of the node. The expected change in the probability  $p_i(1, z, t)$  for node  $i$  is obtained by integration:

$$\begin{aligned}
E[p_i(1, t + 1) - p_i(1, t)] &= \int_{\mathbb{R}} p_z(z(t)) p(1|0; z) p_i(0, z, t) dz \\
&\quad - \int_{\mathbb{R}} p_z(z'(t)) p(0|1; z'_i) p_i(1, z', t) dz'.
\end{aligned} \tag{43}$$

To avoid any confusion with the notation, we recall that  $p_z$  is the density function of the net fragility  $z$ , while  $p(1|0; z)$  is the probability that a node with net fragility  $z$  switches from state 0 to state 1, and finally  $p_i(0, z, t)$  is the probability that node  $i$  with net fragility  $z$  is in state 0 at time  $t$ .

We now average both sides of the equation above across nodes. In particular, the average of the r.h.s. yields

$$\begin{aligned}
&\int_{\mathbb{R}} p_z(z(t)) p(1|0; z) \frac{1}{n} \sum_i p_i(0, z, t) dz \\
&\quad - \int_{\mathbb{R}} p_z(z'(t)) p(0|1; z') \frac{1}{n} \sum_i p_i(1, z', t) dz'.
\end{aligned} \tag{44}$$

Noticing that, for large  $n$

$$\begin{aligned}
X(t) &= \frac{1}{n} \sum_i p_i(1, z, t) \\
1 - X(t) &= \frac{1}{n} \sum_i p_i(0, z, t)
\end{aligned} \tag{45}$$

we get

$$\begin{aligned}
X(t + 1) - X(t) &= (1 - X(t)) \int_{\mathbb{R}} p_z(z(t)) p(1|0; z(t)) dz \\
&\quad - X(t) \int_{\mathbb{R}} p_z(z'(t)) p(0|1; z') dz'.
\end{aligned} \tag{46}$$

Equation (46) describes the dynamics of the expected fraction of failures in a system with both heterogeneity of threshold,  $\theta$ , or fragility,  $\phi$ , and with stochasticity in the cascading mechanism. We can now obtain mean-field equations for various existing models, by specifying (1) the transition probabilities  $p(1|0; z)$  and  $p(0|1; z')$ , and (2) the distribution  $p_\theta(\theta)$  for the thresholds  $\theta_i$ .

### 5.3 Recovering Deterministic Cascade Models

In order to recover the deterministic models of Section 3, we first notice that in those cases the transition from state  $s = 0$  to  $s = 1$  is not really conditional to the state at previous time. Actually, in these models a node changes to a certain state with a probability which is independent of its current state. We emphasize, however, that our framework is general enough to cover cases in which failure is really conditional on  $s$ .

For the models discussed in Section 3, we can assume  $\theta' = \theta$  and thus  $z' = z$ , and further  $\beta = \beta'$ ,  $\gamma = \gamma' = 1$ . We have then

$$\begin{aligned} p(1|0; z) &= p(1|1; z) = p(1; z) \\ p(0|1; z) &= p(0|0; z) = p(0; z). \end{aligned} \quad (47)$$

We now set  $\beta \rightarrow \infty$ , which implies that the transition probability in Equation (42) tends to the Heaviside function:

$$p(1|0; z) = \Theta(z); \quad p(0|1; z) = \Theta(-z) \quad (48)$$

Since, for any real function  $g$  holds

$$\int_{\mathbb{R}} g(x)\Theta(x)dx = \int_0^{\infty} g(x)dx, \quad (49)$$

we obtain

$$\begin{aligned} X(t+1) - X(t) &= (1 - X(t)) \int_0^{\infty} p_z(z(t))dz \\ &\quad - X(t) \int_{-\infty}^0 p_z(z(t))dz. \end{aligned} \quad (50)$$

Because of  $\int_{-\infty}^0 p_z(z(t))dz + \int_0^{\infty} p_z(z(t))dz = 1$ , this finally yields

$$X(t+1) = \int_0^{\infty} p_z(z(t))dz \quad (51)$$

Eqn. (51) coincides with Eqn. (3).

### 5.4 Recovering Stochastic Models with Homogeneous Threshold

In order to recover models of herding and stochastic contagion, we instead keep the stochastic nature of the failure but we assume that the failure threshold is the same across nodes,  $\theta_i = \theta$ ,  $\forall i$ . In a mean field approximation, we replace the individual fragility with the average one, so that also  $z_i$  is constant across the nodes  $z_i = z \forall i$ . Then the probability density of  $z$  in Equation

(46) is equivalent to a delta function and the integral over  $dz$  drops. The macroscopic mean-field equation then reads

$$X(t+1) - X(t) = (1 - X(t))p(1|0; z) - X(t)p(0|1; z) \quad (52)$$

Eqs. (52) will be the starting point for discussing specific contagion models in Sections 5.5, 5.6.

## 5.5 Voter Model

The linear voter model (LVM) is a very simple model of herding behavior. The dynamics is given by the following update rule: a voter, i.e. a node  $i \in A$  of the network, is selected at random and adopts the state of a randomly chosen nearest neighbor  $j$ . After  $n$  such update events, time is increased by 1. The probability to choose a node  $j$  in state 1 from the neighborhood of node  $i$  is proportional to the frequency of nodes with state 1 in that neighborhood,  $f_i$  (and conversely for state 0). Consequently, the transition probability towards the opposite state is proportional to the local frequency of the opposite state. It is also independent of the current state of the node.

$$\begin{aligned} p(1) &= p(1|1) = p(1|0) = f_i \\ p(0) &= p(0|0) = p(0|1) = 1 - f_i \end{aligned} \quad (53)$$

In order to match this dynamics within our framework, we consider values of  $\beta$  of the order of 1. From Equation (42), we obtain in linear approximation:

$$\begin{aligned} p(1|0, z_i) &= \frac{\gamma}{2} [1 + \beta z_i] \\ p(0|1, z_i) &= \frac{\gamma'}{2} [1 - \beta' z_i']. \end{aligned} \quad (54)$$

With  $\theta_i = \theta'_i$ ,  $\beta = \beta'$ ,  $\gamma = \gamma'$ , this matches the transition probabilities for the LVM provided that:

$$\begin{aligned} \gamma [1 + \beta(\phi - \theta_i)] &= 2f_i \\ \gamma [1 - \beta(\phi - \theta_i)] &= 2(1 - f_i) \end{aligned} \quad (55)$$

This is realized by choosing

$$\gamma = 1; \beta = 2; \theta = \frac{1}{2} \Rightarrow \phi_i = f_i \quad (56)$$

We note that the threshold  $\theta$  coincide with the unstable equilibrium point of the LVM,  $1/2$ , that distinguishes between minorities and majorities in the neighborhood. The fragility equals the local frequencies  $f_i$  of infected nodes, and does not depend on the node itself. If a majority

of nodes in the neighborhood has failed, this more likely leads to a failed state of node  $i$ ; if the failed nodes are the minority, this can lead to a transition into the healthy state. Since the fragility coincides with fraction of neighbours in state 1 (or 0), VM fits in the first model class described in Sec. 3.1, with the specificity that the failure process is stochastic and the threshold is homogeneous across nodes.

As a consistency check, if we assume for one moment the failure process to be deterministic, one could directly apply Eqn. (27). Since the probability distribution of the threshold would be trivially a delta function  $\delta_{1/2}(\theta)$ , its cumulative distribution would be the Heaviside function  $P_\theta(X) = \Theta(X - 1/2)$ . This would imply that the dynamics reaches  $X^* = 1$  as stable fix point as soon as  $X(0) > 1/2$  and viceversa for  $X^* = 0$ .

Coming back to the usual stochastic VM, in order to obtain the mean-field dynamics, we now approximate  $f_i(t)$  with  $X(t)$ , i.e. we replace  $p(1|0, z) = X(t)$ ,  $p(0|1, z) = 1 - X(t)$  in Equation (52). This recovers the well known mean-field dynamics of the LVM,  $dX/dt = 0$ , i.e. the expected asymptotic fraction of failures (which differs from the individual realizations) coincide with the initial fraction  $X(0)$  of failed nodes.

With a similar procedure we can also account for nonlinear VM [27], in which the probability to switch to a failed or healthy state is a non-linear function of the fraction of failed nodes in the neighborhood:

$$\begin{aligned} p(1|0; z_i) &= p(1) = f_i(t) F_1(f_i(t)) \\ p(0|1; z_i) &= p(0) = (1 - f_i(t)) F_2(f_i(t)) \end{aligned} \quad (57)$$

$F_1$  and  $F_2$  are frequency dependent functions which describe the non-linear response of a node on the fraction of failed nodes in the neighborhood. If we again replace  $f_i$  with the global frequency of failures  $X$ , we arrive at the macroscopic dynamics in mean-field limit:

$$X(t+1) - X(t) = (1 - X(t)) X(t) [F_1(X) - F_2(X)] \quad (58)$$

In the linear case  $F_1 = F_2 = 1$ , the prediction for the expected value of  $X$  does not give sufficient information about individual realizations of the Voter dynamics. In fact, it is well known that the global outcome of the LVM leads to global failure with a probability equal to the initial fraction of infected nodes,  $X(0)$ . In other words, if we run a simulation with e.g.  $X(0) = 0.3$  for 100 times, then in 30 cases we will reach a state of global failure, whereas in 70 cases, no failure at all will prevail. This differs from the case of the cascading models described in Sect. 3, in which the mean field dynamics gives us some more information about individual realizations.

In the non-linear case ( $F_1 \neq 1$ ,  $F_2 \neq 1$ ), different scenarios arise depending on the nonlinearity. In [27] it was shown that even a small non-linearity may lead to either states where global failure is always reached, or to states with a coexistence of failed and healthy nodes. It is worth noticing

that both of these scenarios are obtained with *positive frequency dependence*, i.e. a transition probability to fail that increases monotonically with the local frequency  $f$ . Thus, small deviations in the nonlinear response can either enhance systemic risk, or completely prevent it.

## 5.6 SIS-SI model

The SIS model [33] is the most known model of epidemic spreading. On the microlevel, healthy nodes get infected with probability  $\nu$  if they are connected to one or more infected nodes. In other words, the parameter  $\nu$  measures the infectiousness of the disease in case of contact with an infected node. This means that the effective transition probability of node  $i$  from healthy to infected state is proportional to the probability  $q$  that a neighbour is infected times the degree  $k_i$  of the node. Indeed, the larger the number of contacts, the more likely it is to be in contact with an infected node. On the other hand, failed nodes recover spontaneously with probability  $\delta$ . The transition probabilities are then as follows:

$$p(1|0, z_i) = \nu k_i q; \quad p(0|1) = \delta \quad (59)$$

with  $0 \leq \nu \leq 1$ . We do not redefine, as usually done, the infection rate as  $\lambda = \nu/\delta$  with  $\delta = 1$ , because we want to cover the case  $\delta = 0$ , as we will see below.

We interpret of course infection state as failure state. Matching the transition probabilities of SIS with the ones in our framework, we obtain:

$$\begin{aligned} \gamma [1 + \beta(\phi - \theta_i)] &= 2\nu k_i q \\ \gamma' [1 - \beta'(\phi - \theta'_i)] &= 2\delta \end{aligned} \quad (60)$$

This implies that our framework recovers the transition probabilities of the SIS model, provided that:

$$\begin{aligned} \gamma = 1 \quad ; \quad \beta = 2 \quad ; \quad \theta = \frac{1}{2} &\Rightarrow \phi_i = \nu k_i q \\ \gamma' = 2\delta \quad ; \quad \beta' = 0 & \end{aligned} \quad (61)$$

In order to understand the relation of SIS with the other models, we can approximate the probability  $q$  that a node fails with the fraction of failed neighbours  $f_i$ . The resulting expression for the fragility,  $\phi_i = \nu k_i f_i$ , is proportional to the fraction of failed nodes as in model class (i) of Sec. 3.1. However, the term  $k_i$  implies that the infection probability grows with the number of connections in the network. This feature makes the biggest difference between the SIS model and the cascade models studied in the previous sections, apart of course from the fact that the contagion process is stochastic and the threshold homogeneous. Another important feature that

emerges is the asymmetry in the transition probabilities between healthy and failed state and backwards.

In order to derive a macroscopic dynamics, we apply the mean-field approximation  $f_i \sim q \sim X$  and we assume a homogeneous network with  $k_i = k$  for all nodes. Starting from Equation (52), we obtain

$$X(t+1) - X(t) = \nu k X(t)(1 - X(t)) - \delta X(t) \quad (62)$$

The last negative term in the R.H.S. of Eqn. (62) implies that there is no global spreading of infection if  $\nu < \nu_c = \frac{\delta}{k}$  and the only stable fix point is  $X^* = 0$ . For  $\nu \geq \nu_c$  there is a unique stable fix point with  $X^* > 0$ .

As it is well known, the existence of a critical infection rate  $\nu_c$  does not hold, however, if, instead of the mean-field limit with homogeneous degree, a heterogeneous degree distribution of the nodes is assumed [33]. The implications of degree heterogeneity and degree-degree correlation in epidemic spreading have been investigated in a number of works [5].

The SI model, in which no transition into the healthy state is possible, is recovered setting additionally  $\delta = 0$ . We then obtain the logistic growth equation:

$$X(t+1) - X(t) = \nu k X(t)(1 - X(t)) \quad (63)$$

where  $X(t) = 1$  is the only stable fix point of the dynamics. Any initial disturbance of a healthy state eventually leads to complete infection.

We conclude by noting that, despite its simplicity, the SI model has been used to describe a number of real contagious processes, such as the spread of innovations [16] or herding behavior in donating money [29]. In the latter case, the mean-field interaction was provided by the mass media. In other words, because of the constant and homogeneous information about other people's donations, the individual transition depends on the global (averaged) frequency of donations instead of the local one. Interestingly, it could be shown that in the particular example of 'epidemic' donations, the time scale depends itself on time, indicating a slowing down of the dynamics due to a decrease in public interest.

## 6 Conclusion

In this paper, we wish to clarify the meaning and the emergence of systemic risk in networks with respect to several existing models. To unify their description, we propose a framework in which nodes are characterized (1) by a discrete failure state  $s_i(t)$  (healthy or failed) and (2) by a continuous variable, the *net fragility*,  $z_i(t)$ , capturing the difference between fragility  $\phi_i$  of the



node and its failing threshold  $\theta_i$ . By choosing an appropriate definition of fragility in terms of the failure state and/or the fragility of neighbouring nodes, we are able to recover, as special cases, several cascade models as well as contagion models previously studied in the literature.

Our paper contributes to the investigation of these models in several ways. First of all, we have provided a novel framework to cover both cascade and contagion models in a deterministic approach, which is further suitable to be generalized also to the stochastic case. Secondly, our framework allows us to unify a number of existing, but seemingly unrelated models, pointing out to their commonalities and differences. Thirdly, we are able to identify three different model classes, which are each characterized by a specific mechanism of transferring fragility between different nodes. These are (i) 'constant load', (ii) 'load redistribution', and (iii) 'overload redistribution'.

Systemic risk, within our framework, is defined as the stable fraction of failed nodes  $X^*$  in the system. As  $X^* = 1$  denotes the complete breakdown of a system, we are interested in trajectories of the system where  $X^*$  is much below one. In order to determine these trajectories, in this paper we derive a *macroscopic dynamics* for  $X(t)$  based on the microscopic dynamics. As a major contribution of this paper, we are able to find, for each of the three classes, macroscopic equations for the final fraction of failed nodes in the mean-field limit.

In order to compare the systemic risk between the three classes, we have studied the macroscopic dynamics of each of them with the same initial conditions. Most importantly, we found that the differences on the microscopic level translate into important differences on the macroscopic level, which are visualized in a phase diagram of systemic risk. This indicates, for each of the model classes, which given initial conditions result into what total fraction of failure. This way we could verify that, for instance, in class (ii) there is a first-order transition between regions of high systemic risk and regions with low systemic risk. In contrast, class (i) displays such a sharp transition only in some smaller part of the phase space, while class (iii) does not display any abrupt transition at all. Such an insight helps us to understand whether and for which parameters small variations of initial conditions may lead to an abrupt collapse of the whole system, in contrast to a gradual increase of systemic risk.

In addition to the macro dynamics, we have also investigated the different model classes on the microscopic level. A number of network examples made clear how the different transfer mechanisms affect the microdynamics of cascades. As an interesting insight, we could demonstrate that the role of nodes with high degree change depending on type of load transfer. In the inwards variant of first class model, high degree nodes are more protected from contagion, whereas in the outwards variant of the same class, they become more exposed to contagion if they are connected to many low degree nodes (which holds for disassortative networks). Furthermore, we could point out that the results strongly depend on the position of the initially failing node. A systematic analysis identifying the crucial nodes from a systemic risk point of view is left for future work.

Finally we have extended our general framework so to encompass models of stochastic contagion, as known from VM and SIS. Both of these models belong to the first class, but differently from the models studied in Section 3.1, the threshold is homogeneous and the failure is stochastic. Hence, it becomes more clear how these established models of herding behavior and epidemic spreading are linked to the ‘cascade’ models discussed in the literature.

Our work could be extended in several ways. First, one could apply techniques to deal with heterogeneous degree distributions to the three classes of cascading model, introduced in Sec. 3. This could be carried out also in the presence of degree-degree correlation, as recently discussed for contagion models [5]. Furthermore, one could investigate more in detail the case of both heterogeneous threshold and stochastic failures. Compared to the simple SIS, it seems more realistic to assume that the probability of contagion depends on an intrinsic heterogeneous property of the nodes (the threshold). Such heterogeneity could also play a crucial role, as it has been found for the heterogeneity in the degree [33].

A last remark is devoted to the discussion of systemic risk. In our paper, we have provided mean-field equations to calculate the total fraction of failed node in a system, which we regard as a measure of systemic risk. This implies that systemic risk is associated with a system state of global failure, i.e. there is no ‘risk’ anymore, as almost all nodes already failed. In contrast, it could be also appropriate to define ‘systemic risk’ as a situation, where the system has not failed yet, but small changes in the initial conditions or fluctuations during the evolution may lead to its complete collapse. Our general framework has already contributed insight into this problem, by identifying those areas in the (mean-field) phase diagram where we can observe a sharp transition between a globally healthy and a globally failed system. This is related to precursors of a crisis as it identifies parameter constellations to make a system vulnerable that looks apparently healthy. On the other hand, using our approach we were able to assess that for certain transfer mechanisms such an abrupt change in the global state is not observed at all – which means that systems operating under some conditions are less vulnerable to small changes.

## Acknowledgements

This work is part of a project within the COST Action P10 “Physics of Risk”. J.L. and F.S. acknowledge financial support from the Swiss State Secretariat for Education and Research SER under the contract number C05.0148. S.B. and F.S. acknowledge financial support from the ETH Competence Center ‘Coping with Crises in Complex Socio-Economic Systems’ (CCSS) through ETH Research Grant CH1-01-08-2.

## References

- [1] Avellaneda, M.; Zhu, J. (2001). Distance to default. *Risk* **14(12)**, 125–129.
- [2] Battiston, S.; Gatti, D. D.; Gallegati, M.; Greenwald, B. C. N.; Stiglitz, J. E. (2007). Credit Chains and Bankruptcies Avalanches in Production Networks. *Journal of Economic Dynamics and Control* **31(6)**, 2061–2084.
- [3] Battiston, S.; Gatti, D. D.; Gallegati, M.; Greenwald, B. C. N.; Stiglitz, J. E. (2009). Liaisons Dangereuses: Increasing Connectivity, Risk Sharing and Systemic Risk. *forthcoming* .
- [4] Bianconi, G.; Marsili, M. (2004). Clogging and self-organized criticality in complex networks. *Physical Review E* **70(3)**, 35105.
- [5] Boguná, M.; Pastor-Satorras, R.; Vespignani, A. (2003). Absence of epidemic threshold in scale-free networks with degree correlations. *Physical review letters* **90(2)**, 28701.
- [6] Brunnermeier, M. (2008). Deciphering the 2007-08 Liquidity and Credit Crunch. *Journal of Economic Perspectives* .
- [7] Carreras, B.; Lynch, V.; Dobson, I.; Newman, D. (2004). Complex dynamics of blackouts in power transmission systems. *Chaos: An Interdisciplinary Journal of Nonlinear Science* **14**, 643.
- [8] Caruso, F.; Latora, V.; Pluchino, A.; Rapisarda, A.; Tadić, B. (2006). Olami-Feder-Christensen model on different networks. *The European Physical Journal B-Condensed Matter* **50(1)**, 243–247.
- [9] Crucitti, P.; Latora, V.; Marchiori, M. (2004). Model for cascading failures in complex networks. *Physical Review E* **69**, 045104.
- [10] Dodds, P.; Payne, J. (2009). Analysis of a threshold model of social contagion on degree-correlated networks. *Phys Rev E* **79**, 066115.
- [11] Dodds, P.; Watts, D. (2004). Universal behavior in a generalized model of contagion. *Physical Review Letters* **92(21)**, 218701.
- [12] Eisenberg, L.; Noe, T. (2001). Systemic Risk in Financial Systems. *Management Science* **47(2)**, 236–249.
- [13] Goh, K.; Lee, D.; Kahng, B.; Kim, D. (2003). Sandpile on Scale-Free Networks. *Physical Review Letters* **91(14)**, 148701.

- [14] Gómez-Gardeñes, J.; Latora, V.; Moreno, Y.; Profumo, E. (2008). Spreading of sexually transmitted diseases in heterosexual populations. *Proceedings of the National Academy of Sciences* **105(5)**, 1399.
- [15] Granovetter, M. (1978). Threshold Models of Collective Behavior. *American Journal of Sociology* **83(6)**, 1420.
- [16] Jackson, M.; Rogers, B. (2007). Relating Network Structure to Diffusion Properties through Stochastic Dominance. *The BE Journal of Theoretical Economics* **7(1)**, 1–13.
- [17] Kahng, B.; Batrouni, G.; Redner, S.; de Arcangelis, L.; Herrmann, H. (1988). Electrical breakdown in a fuse network with random, continuously distributed breaking strengths. *Physical Review B* **37(13)**, 7625–7637.
- [18] Kim, D.; Kim, B.; Jeong, H. (2005). Universality Class of the Fiber Bundle Model on Complex Networks. *Physical Review Letters* **94(2)**, 25501.
- [19] Kinney, R.; Crucitti, P.; Albert, R.; Latora, V. (2005). Modeling cascading failures in the North American power grid. *The European Physical Journal B-Condensed Matter and Complex Systems* **46(1)**, 101–107.
- [20] König, M. D.; Battiston, S.; Napoletano, M.; Schweitzer, F. (2008). On Algebraic Graph Theory and the Dynamics of Innovation Networks. *Networks and Heterogeneous Media* **3(2)**, 201–219.
- [21] Kun, F.; Zapperi, S.; Herrmann, H. (2000). Damage in fiber bundle models. *The European Physical Journal B-Condensed Matter and Complex Systems* **17(2)**, 269–279.
- [22] Lorenz, J.; Battiston, S. (2008). Systemic risk in a network fragility model analyzed with probability density evolution of persistent random walks. *Netw. Heterog. Media* **3(2)**, 185.
- [23] Moreno, Y.; Gomez, J.; Pacheco, A. (2002). Instability of scale-free networks under node-breaking avalanches. *Europhysics Letters* **58(4)**, 630–636.
- [24] Morris, S.; Shin, H. (2008). Financial Regulation in a System Context. *Brookings Panel on Economic Activity, September* .
- [25] Motter, A. (2004). Cascade Control and Defense in Complex Networks. *Physical Review Letters* **93(9)**, 98701.
- [26] Pastor-Satorras, R.; Vespignani, A. (2001). Epidemic Spreading in Scale-Free Networks. *Physical Review Letters* **86(14)**, 3200–3203.

- [27] Schweitzer, F.; Behera, L. (2009). Nonlinear voter models: the transition from invasion to coexistence. *The European Physical Journal B* **67(3)**, 301–318.
- [28] Schweitzer, F.; Fagiolo, G.; Sornette, D.; Vega-Redondo, F.; Vespignani, A.; White, D. R. (2009). Economic Networks: The New Challenges. *Science* **325(5939)**, 422–425.
- [29] Schweitzer, F.; Mach, R. (2008). The epidemics of donations: Logistic growth and power-laws. *PLoS ONE* **3(1)**.
- [30] Sornette, D. (2009). Dragon-Kings, Black Swans and the Prediction of Crises. *forthcoming on International Journal of Terraspace Science and Engineering, arXiv:0907.4290* .
- [31] Sornette, D.; Andersen, J. (1998). Scaling with respect to disorder in time-to-failure. *The European Physical Journal B-Condensed Matter and Complex Systems* **1(3)**, 353–357.
- [32] Stark, H.; Tessone, C.; Schweitzer, F. (2008). Decelerating microdynamics can accelerate macrodynamics in the voter model. *Physical Review Letters* **101(1)**, 18701.
- [33] Vespignani, A.; Pastor-Satorras, R. (2002). Epidemic Spreading on Scale-free Networks. *Physical Review E* **65**, 035108.
- [34] Vespignani, A.; Zapperi, S. (1998). How self-organized criticality works: A unified mean-field picture. *Phys. Rev. E* **57(6)**, 6345–6362.
- [35] Watts, D. (2002). A Simple Model of global cascades on random networks. *Proceedings of the National Academy of Sciences* **99(9)**, 5766.

## A Eisenberg-Noe model

An interesting model of contagion which has not been investigated in the econophysics literature is the one developed by Eisenberg and Noe [12]. It introduces a so called fictitious default algorithm as a clearing mechanism in a financial system of liabilities. When some agents in the system cannot meet fully their obligations, the task of computing how much each one owes to the other becomes nontrivial in presence of cycles in the network of liabilities.

The basic assumptions of the clearing mechanism are (i) limited liability (a firm need not spend more than it has), (ii) absolute priority of debt over cash (a firm has to spend all available cash to satisfy debt claims first), (iii) no seniority (all claims have the same priority).

A financial system of  $n$  firms is described by a vector of total obligations  $x^0$ , a matrix of relative liabilities  $A$ , and a vector of operating cash flows  $\theta$ .  $x_i^0$  is the total amount of liabilities firm  $i$  has

towards other firms,  $a_{ij}$  specifies what fraction of its own total obligations firm  $i$  owes to firm  $j$ , and  $\theta_i$  determines the liquid amount of money of firm  $i$ . Thus,  $a_{ij}x_i^0$  is the nominal liability  $i$  has to  $j$ . The matrix  $A$  is row-stochastic, which means all entries are non-negative and rows sum up to one. This condition ensures that individual obligations sum up to the total obligations  $x_j^0$ . The expected payments to firm  $i$  from its debtors is thus:

$$(A^T x^0)_i = \sum_{j=1}^n a_{ji}x_j^0 \quad (64)$$

If it happens that the total cash flow, i.e., the expected repayments of others plus operating cash-flow, is less than the total obligations, i.e.

$$\theta_i + \sum_{j=1}^n a_{ji}x_j^0 < x_i^0 \quad (65)$$

firm  $i$  cannot meet its obligation in full and defaults. This implies a reduction of the expected payments to its creditors, which might in turn default as a second-order effect, and so on. This makes this model close to the class of overload redistribution because the expected payments of a node do not vanish entirely when it fails.

The fictitious default algorithm defined in [12] consists of finding a clearing vector  $x^*$  of total payments which fulfills the equation

$$x_i = \min\{\theta_i + \sum_{j=1}^n a_{ji}x_j, x_i^0\} \quad (66)$$

for all  $i$ . As shown in [12], using mild assumptions, such a clearing vector exists and is unique and the fictitious default algorithm, with  $x(0) = x^0$ , is well defined. The sequence  $x(t)$  represents a decreasing sequence of clearing vector candidates which terminates in at most  $n$  steps at the clearing vector. The new clearing vector candidate  $x(t+1)$  is computed from a given candidate  $x(t)$  taking into account the first order defaults given clearing vector candidate  $x(t)$ , but not the second order defaults. These are checked in the successive time steps.

Following our general framework presented in Section 2, we can define fragility as

$$\phi_i(x(t), x^0, A) = x_i^0 - \sum_{j=1}^n a_{ji}x_j(t) \quad (67)$$

which is the amount of debt which has to be covered by the operating cash flow  $\theta_i$ , given the current candidate for the clearing vector  $x(t)$ . From  $x(t)$ ,  $x^0$ ,  $A$ , and  $\theta$  we can determine the failing state  $s_i(t+1)$  as in Equation (2) as

$$s_i(t+1) = \Theta(\phi_i(x(t), x^0, A) - \theta_i). \quad (68)$$

Given a clearing vector candidate  $x(t)$ , the *value of the equity* of firm  $i$  is given by

$$\theta + \sum_{j=1}^n a_{ji}x_j(t) - x_i(t) \quad (69)$$

which is the operating cash flow plus the expected amount of payments received by others minus the payment to others which are possible, given the currently expected payments from the other. A new clearing vector candidate  $x(t+1)$  is computed from  $x(t)$  by determining the failing state  $s(t+1)$ . This leads to a simple fix point equation (see Eisenberg and Noe [12, p. 243]), which usually has a unique fix point. That means, the fictitious default algorithm is constituted in such a way that it solves a system of linear equations. If successful, the algorithm runs until a clearing vector is found which gives that the value of the equity is zero (and not negative) for a firm in default, and positive for a non-defaulting firm. At least one non-defaulting firm should be found by the fictitious default algorithm, which means that there is at least one firm  $i$  for which it holds  $x_i(t) = x_i^0$  holds. If not, then the clearing vector candidates diverge toward  $-\infty$ , and the algorithm fails. This represents a full break down of the financial system.

The relation between this model and our third model class is not straightforward because the new clearing vector candidate  $x(t)$  is not necessarily always uniquely defined by the current fragility  $\phi(t)$  as given in (67). Therefore, we chose to study the simpler models in Sec. 3.3.

Investigating the macro-perspective as in Section 4, one finds that the Eisenberg-Noe model can be approximated by the macroscopic equation for the overload redistribution. The approximations would be fairly good when the system is close to a fully connected network (everybody borrows equally from everybody else) and uncorrelated operating cash flows.

## B Further examples

Section 3 has pointed out that the propagation of cascades, in addition to the mechanism of transfer, strongly depends on the initial condition, in particular on the position of the first failing node. In order to further illustrate this important point, we present additional examples with a different initially failing node. All these examples start from the setup shown in Figure 1. Their outcome should be compared to the respective examples discussed in Figures 2, 3, 4

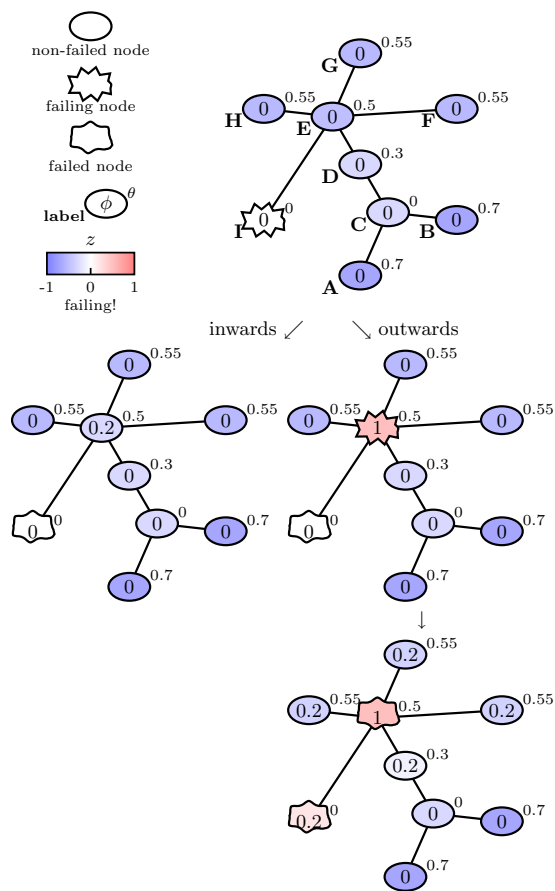


Figure 13: **Constant damage.** Example to be compare with Figure 2. Here, node **I** initially fails.



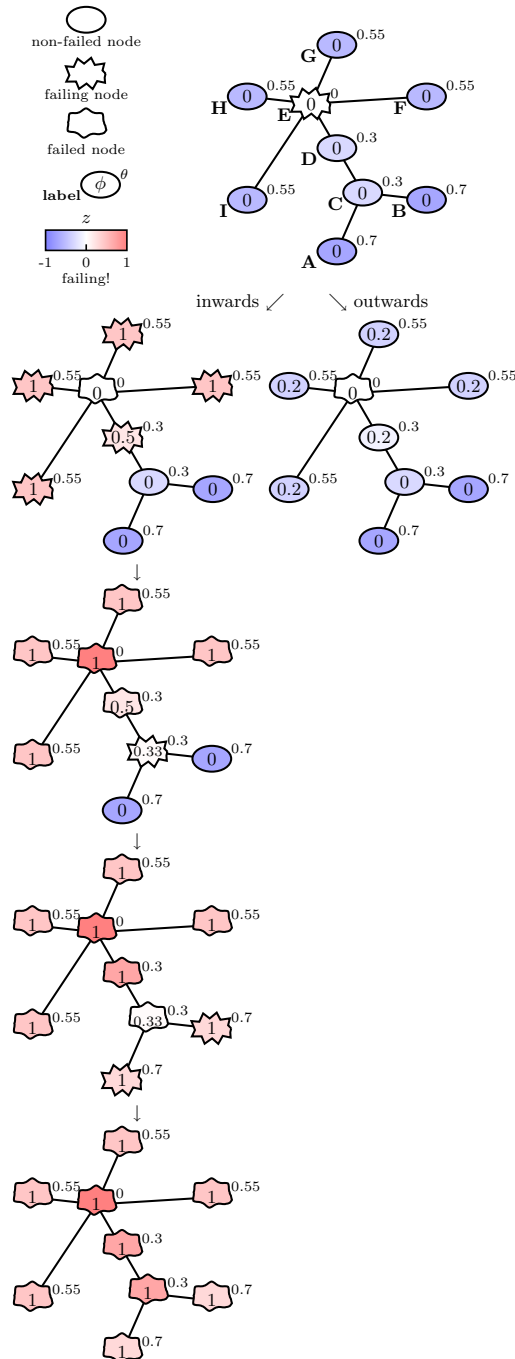


Figure 14: **Constant damage.** Example similar to the one in Figure 13 but with highest degree node **E** failing initially. The example clearly shows a difference in the spreading properties of hubs: in the ‘inwards variant’ the hub spreads failures to low-degree nodes; the opposite for the ‘outwards variant’.

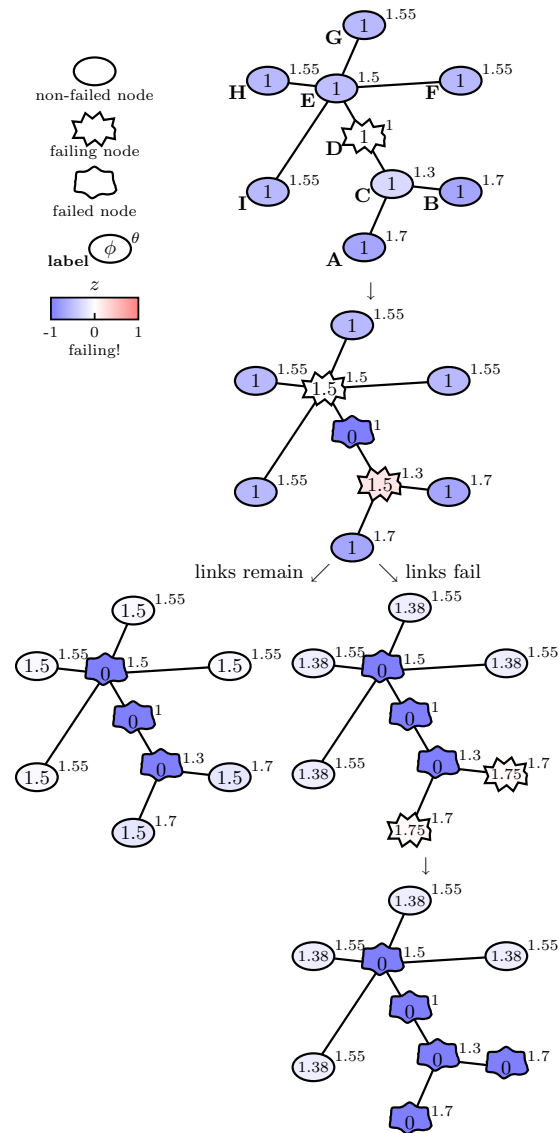


Figure 15: **Load redistribution.** Compare with Fig. 3. Here, node **D** fails initially. w.r.t to the previous case, this leads to a propagation of failures in the opposite direction, in the LLSC variant (links fail), while nothing changes in the LLSS variant (links remain).

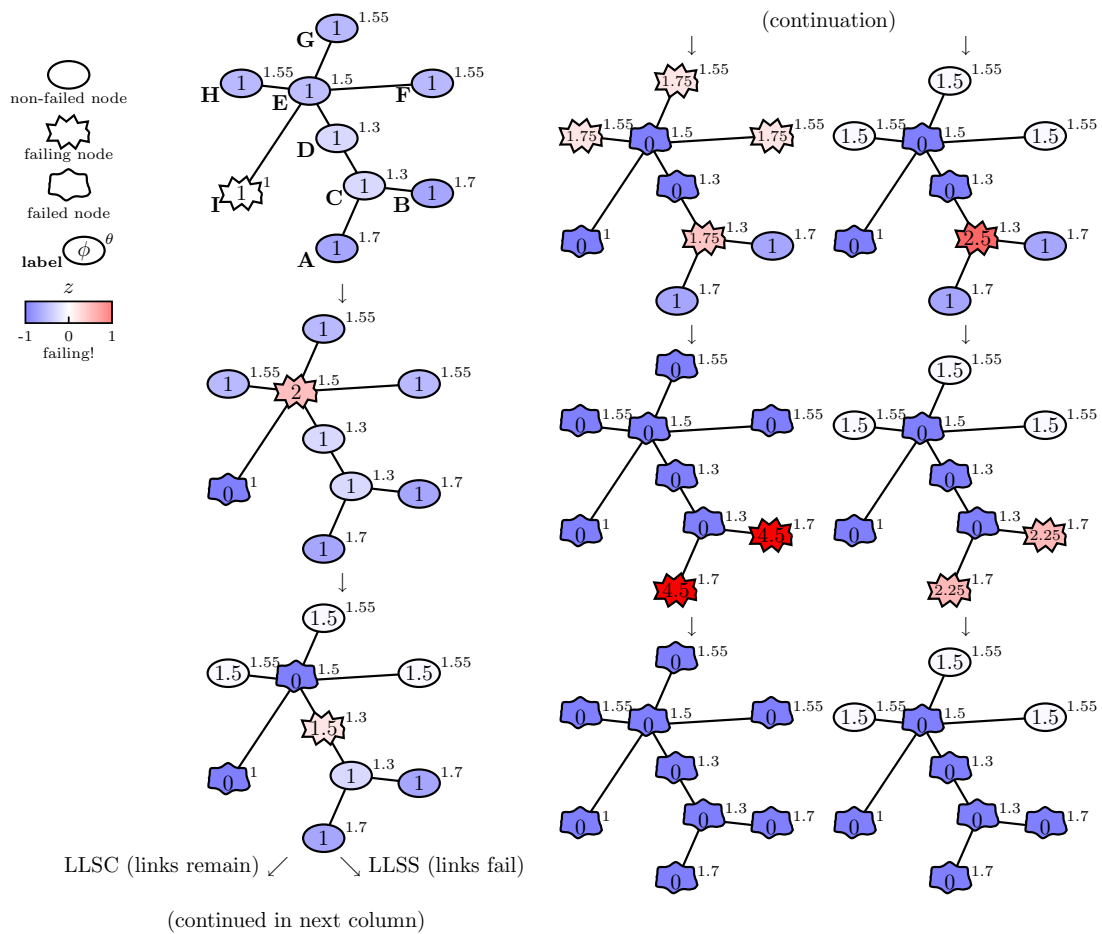


Figure 16: **Load redistribution.** Compare with Figure 3. Here, node **I** fails initially. This leads to full breakdown in the LLSC variant (links remain), while some nodes do not fail in the LLSS variant (links fail) because of a disconnection in the network.